INVESTIGATION OF TECHNIQUES FOR REMOTE MEASUREMENT OF ATMOSPHERIC WIND FIELDS

REPORT NO. 2 PHASE II: ANALYSIS

Contract No. DA-36-039 SC-87293
DA Project No. 3A99-07-001

1 October 1961 - 14 February 1962

M.R.I. Project No. 2510-E

For

U. S. Army Signal Research and
Development Laboratory
Fort Monmouth, New Jersey

Midwest Research Institute
425 Volker Boulevard
Kansas City 10, Missouri

MRI

MIDWEST RESEARCH INSTITUTE

INVESTIGATION OF TECHNIQUES FOR REMOTE MEASUREMENT OF ATMOSPHERIC WIND FIELDS

REPORT NO. 2

Contract No. DA-36-039 SC-87293

Signal Corps Technical Requirement NrSCL-5825
dated 9 November 1960

PHASE II: ANALYSIS

15 October 1961 to 14 February 1962

M.R.I. Project No. 2516-E

The object of this phase of the study is the analysis of three possible methods of remote wind field measurement:

1. Scattering from natural atmospheric turbulence,
2. Electromagnetic scattering from acoustic waves, and
3. Infrared tracking of an artificially heated "bubble."

Report prepared by R. W. Fetter, P. L. Smith, Jr., B. L. Jones, H. F. Schick, and R. M. Stewart, Jr.

PREFACE

Work on this project has been under the leadership of Mr. R. W. Fetter. The analyses have been done by Dr. P. L. Smith, Jr., Dr. R. M. Stewart, Jr., Mr. H. F. Schick, and Mr. B. L. Jones. Mr. P. C. Constant, Jr., Head, Electronics Engineering Section, has supervised the project.

Approved for:

MIDWEST RESEARCH INSTITUTE

Warren E. Snyder

Warren E. Snyder, Director
Engineering Division

26 February 1962

bc

TABLE OF CONTENTS

TABLE OF CONTENTS (Continued)

List of Tables

TABLE OF CONTENTS (Concluded)

List of Illustrations

PURPOSE

The purpose of this program is to investigate any methods, techniques, or equipment which can be used to determine atmospheric wind fields at locations remote from the sensing and measuring apparatus. The work is to be performed in three phases:

I. A survey of the field to ascertain the state-of-the-art through a literature search and a study of current efforts at governmental and non-governmental agencies and institutions;

II. A critical analysis of work done in the field, as found in Phase I, to determine the capabilities of the methods for remote measurements; and

III. The design of experiments to verify the results of the analysis in Phase II.

ABSTRACT

Analyses were made to determine the feasibility of three proposed methods of remote wind measurement using (1) scattering from natural atmospheric turbulence; (2) electromagnetic scattering from acoustic waves; and (3) infrared tracking of an artificially heated volume of air, or "bubble."

Use of natural turbulence as a sensor will require (1) additional data on distribution and characteristics of turbulence from ground level to one mile altitude, (2) correlation of turbulence motion and wind, and (3) radar state-of-the-art improvement to provide consistent detection and measurement.

Remote wind measurements by microwave reflection from acoustic waves have been demonstrated, but additional experimental data are needed to determine maximum usable range and the effects of turbulence on the acoustic waves.

Remote generation of a heated bubble of air does not appear feasible.

I. PUBLICATIONS, LECTURES, REPORTS, AND CONFERENCES

Publications: None

Lectures: None

Reports: Monthly Letter Reports Nos. 5, 6, and 7.

Conferences:

On 8 November 1961, a conference was held at USASRDL, Evans Area, Belmar, New Jersey, with the following persons present: for the Signal Corps -- K. C. Steelman, Contracting Officer's Technical Representative, SMI; H. H. Grote, Project Engineer, SMI; D. A. Deisinger, Chief, Meteorological Division, SM; R. M. Marchgraber, Physicist, SMA; and Dr. H. J. auf'm Kampe, Chief, Atmospheric Physics Branch, SMA: for Midwest Research Institute -- H. L. Stout, Assistant Director, Engineering Division; P. C. Constant, Jr., Head, Electronics Engineering Section; R. W. Fetter, Senior Engineer; and Dr. P. L. Smith, Jr., Senior Engineer.

This conference was held to discuss the results of the first phase as presented in Report No. 1, and the program for Phase II, Analysis. After discussing the nine possible methods suggested for analysis in Report No. 1, it was agreed that only three of these methods would be analyzed to determine their capabilities for remote wind field measurements. These methods are: (1) scattering from natural atmospheric turbulence, (2) electromagnetic scattering from acoustic waves, and (3) infrared tracking of an artificially heated "bubble" of air.

On 19 and 20 February 1962, a conference was held at Midwest Research Institute with Mr. H. H. Grote, Project Engineer, USASRDL, and Messrs. P. C. Constant, Jr., B. L. Jones, and R. W. Fetter of Midwest Research Institute.

Principal subjects discussed were the results of the Phase II investigation, the preparation of this phase report, and the evaluation of the three methods of wind measurement analyzed: (1) electromagnetic scattering from natural turbulence, (2) electromagnetic scattering from acoustic waves, and (3) infrared tracking of an artificially heated bubble. It was tentatively agreed that the use of a heated bubble as a sensor did not merit further investigation. In Phase III, therefore, experiments will be designed only for the wind measuring methods using electromagnetic backscattering from natural turbulence and from acoustic waves.

II. FACTUAL DATA

A. Introduction

A definite Army requirement exists for remote soundings to determine the basic parameters of the atmosphere without the need for probes or material sensors located at, or passing through, the region of interest. The objective of this program, as specified in Technical Requirement Nr SCL-5825, is a study of possible methods for the determination of the wind field of the atmosphere, directly or indirectly, by active or passive means at space coordinates remote from the location of the measuring apparatus.

The first phase of the work was a survey of the literature and organizations in the field to find possible methods of remote wind measurement. Nine proposed methods were found in the survey, but a preliminary analysis, based on the results of other investigators, left only three of these methods for detailed consideration in Phase II, Analysis.

The analyses in this phase have been made to determine the feasibility of using each of the three methods as the basis for a remote wind-measuring instrument. Consideration has been given to such factors as physical parameters involved, the theory of operation, available data, and the state-of-the-art of radar and infrared instrumentation. Where required characteristics are not known, use has been made of mathematical models based on assumed characteristics.

The three methods considered are:

1. Scattering from natural atmospheric turbulence,

2. Electromagnetic scattering from acoustic waves, and

3. Infrared tracking of an artificially heated bubble of air.

The first method has previously been mentioned by various investigators, but no detailed examination has been made. The second method has been demonstrated at short ranges and a general system analysis performed. The third method was suggested by Mr. Harry Moses of Argonne National Laboratory in a discussion during the survey phase and is not known to have been considered previously. Similar analytical procedures would be desirable so that the results could be put on a more common basis for comparison. The variation in parameters used, available information, and previous work done, made it difficult to follow a rigid procedure in the analysis of each method.

B. Scattering from Natural Atmospheric Turbulence

1. Method: One of the most attractive concepts for remote measurement of wind velocities involves the use of reflections of either radar or acoustic signals from the turbulence which exists in the atmosphere. A system making use of such reflections is ideal in that the atmosphere furnishes its own sensor, in the form of turbulent "blobs" or eddies, at the point where the wind velocity is to be measured. In principle, the motion of this turbulent structure only need be observed to ascertain the motion of the adjacent atmosphere. The turbulent "blobs" would be assumed to move along with the mean wind speed. Their velocity would be determined by Doppler techniques, because the transient nature of the turbulent structure makes it unlikely that an ordinary position-tracking system could be used for velocity measurements.

Unfortunately, very little information is available on the actual, detailed characteristics of low level turbulence. This is due partly to the lack of adequate instrumentation and partly to the lack of a pressing demand for such data. Past interest in the subject is well summarized by R. J. Papa[1] in his rather comprehensive survey of atmospheric turbulence:

> "Anemometer recordings illustrate, especially in the lower layers of the atmosphere, that the wind is usually highly irregular. The wind velocity is composed of a complex of oscillations of duration varying from a fraction of a second to many minutes and of an amplitude which is often a substantial fraction of the average speed. The speed of the wind changes not only from instant to instant but also from point to point of space. A complete specification of the velocity field over even a limited portion of the atmosphere is impracticable. The study of atmospheric turbulence is primarily concerned with mean values, such as analysis of the mean distribution of momentum, heat and suspended particles in this rapidly changing field."

If it is assumed that atmospheric turbulence will always be available when needed, there still remain several serious obstacles to any successful development. In particular, there are three basic problems which must be solved before the concept of reflections from natural turbulence can be put to practical use for measuring wind velocities. These are the question of turbulence motion with the wind, the effects of Doppler broadening, and the problem of adequate reflection levels from natural turbulence.

2. The motion of turbulence with respect to the wind: It is assumed that the turbulence in the atmosphere may be characterized by a more-or-less random array of eddies or "blobs." However, these "blobs" will be usable for

wind velocity measurements only if they are carried along, or convected, with a velocity equal to the mean wind velocity, while maintaining essentially uniform structure. There is considerable reason to doubt that this should be so. The turbulence represents a random motion superimposed on the mean motion, and the turbulent "blobs" are believed to be continually growing and dissipating, rather than remaining in a fixed condition.

Some experimental work directed toward a solution to this problem has been conducted at the University of Southampton.[2] The experiments have been directed at establishing whether the turbulent structure in a moving air stream moves with the mean stream velocity. This has been approached by studying the correlation of the measured turbulent fluctuations (of velocity) as a function of downstream distance and time. If the turbulent "blobs" do behave as quasi-permanent bodies which are carried along at the mean stream velocity, these correlation experiments would be expected to show results similar to the curves in Fig. 1, where:

$R(\tau)$ = correlation between quantity as measured at one station and at another station a distance x downstream;

τ = time difference between the measurements at the two stations;

x = distance to downstream station; and

V_s = mean stream velocity.

For example, a correlation between measurements taken at two stations a distance d_1 apart that peaks at a value of 1.0 at time $\tau = d_1/V_s$ indicates that the turbulent structure has remained essentially constant while being convected the distance d_1 with a velocity equal to the mean stream velocity, V_s.

The actual experimental results correspond more closely to Fig. 2. In these curves, the correlation coefficient peaks at a value less than unity, and the peak value decreases as the downstream distance increases. This shows that the turbulent structure is changing with time, and emphasizes the transitory nature of the "blob" structure. In the experiments reported, the value of the peak $R(\tau)$ decreased below 0.5 in 150 μsec. or less. In addition, the peaks occur at times <u>greater</u> than the corresponding d/V values, indicating that the turbulent structure tends to move more slowly than the mean stream velocity.

While these results appear to be discouraging to the wind-measuring application, several points concerning the experimental work should be mentioned. First, the experiments were performed downstream from a jet of air

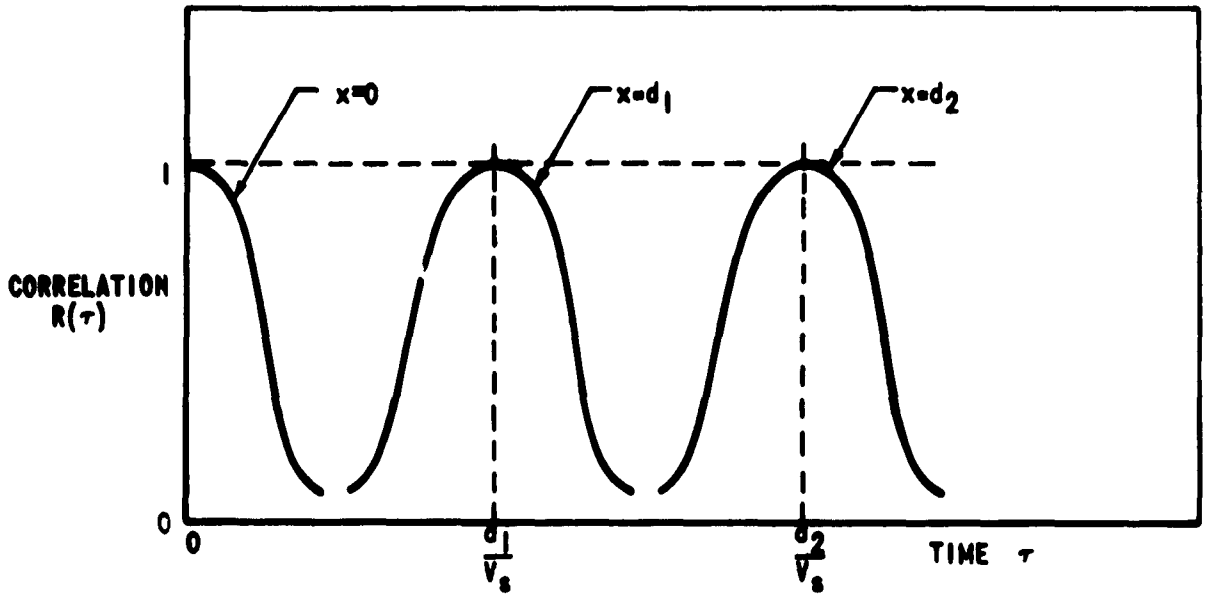

Fig. 1 - Results Expected from Idealized Correlation Experiment

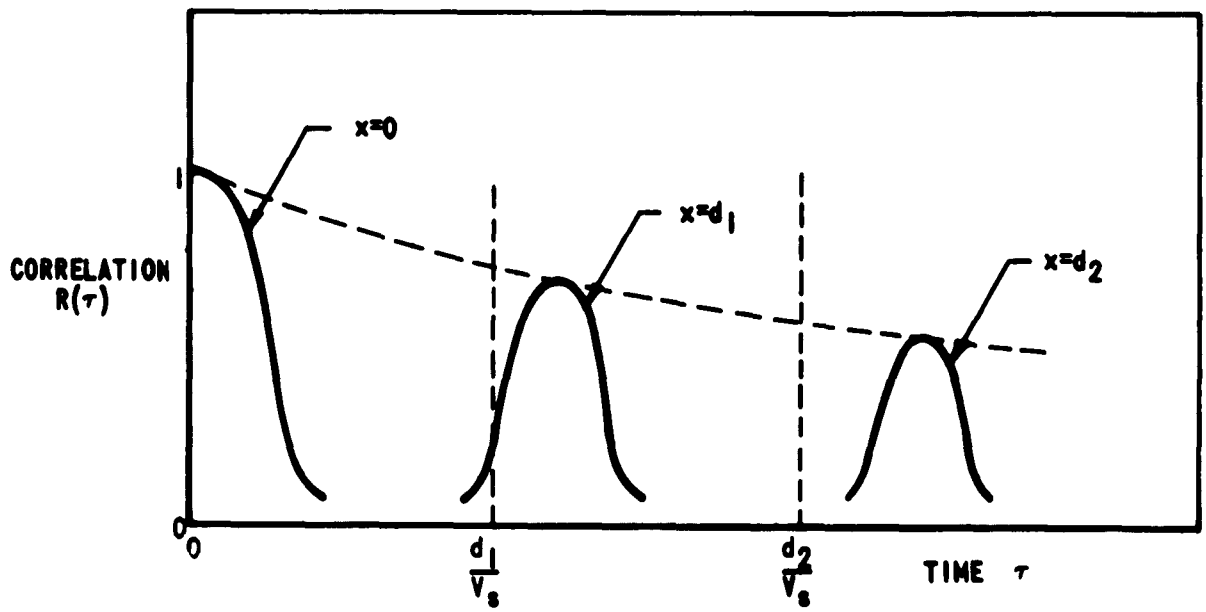

Fig. 2 - Results of Actual Correlation Experiment in a Moving Air Stream (after Richards and Williams[1])

expelled through a 1-in. orifice, and thus it may be questioned whether the results are applicable to turbulence in the free atmosphere. Secondly, the correlation measurements were performed on velocity fluctuations, whereas it is the behavior of the index of refraction fluctuations that is of interest in the electromagnetic reflection problem and that of the acoustic impedance in the acoustic case.

Consequently, it appears necessary to perform similar correlation experiments in the free atmosphere using measurements of refractive index or acoustic impedance before an answer to the problem of convection of turbulence can be given. If a similar decrease of the peak correlation coefficient is observed, there may still be a possibility of using this system, providing the peak $R(\tau)$ remains close to unity for a time τ long enough to permit the required Doppler frequency measurement. If this happens, the subsequent decay of $R(\tau)$ would not affect the operation of the proposed wind-measuring system.

3. The effect of Doppler broadening: Another obstacle to the use of Doppler measurements of turbulence motion with the wind is the effect of the random motion associated with the turbulence. In an idealized situation, the turbulent "blobs" could be regarded as well-defined bodies moving at a uniform velocity with the wind. The spectrum of Doppler frequencies in a signal reflected from the moving "blobs" would then consist of a single line at the frequency corresponding to the wind component along the line of sight. In the actual situation, there is a random turbulent motion superimposed on the mean wind speed. The resulting spectrum of velocities will give rise to a wide spectrum of Doppler frequencies. This effect is illustrated in Fig. 3; a similar phenomenon is the well known Doppler broadening encountered in spectroscopy, where the random thermal motions of the molecules give rise to a broadening of the spectral lines.

The importance of this Doppler broadening effect is difficult to evaluate without some experimental evidence. A set of measurements performed by Emerson Research Laboratories[3] in which the Doppler frequencies in an acoustic signal reflected from atmospheric turbulence were determined provides some evidence of this effect. For wind speeds up to 25 knots, a Doppler spectrum width corresponding to ± 10 knots was not uncommon. While it is not certain that all of this error can be attributed to Doppler broadening, these experiments do at least provide a clue to the possible importance of this effect.

4. The problem of adequate reflection levels from turbulence: The third problem is that of obtaining from atmospheric turbulence a reflected signal which is strong enough to be detected. Although the work by Emerson demonstrated the possibility of detecting acoustic reflections at short ranges (72.5 feet) the experimental configuration was not "remote," but resembled a "forward-

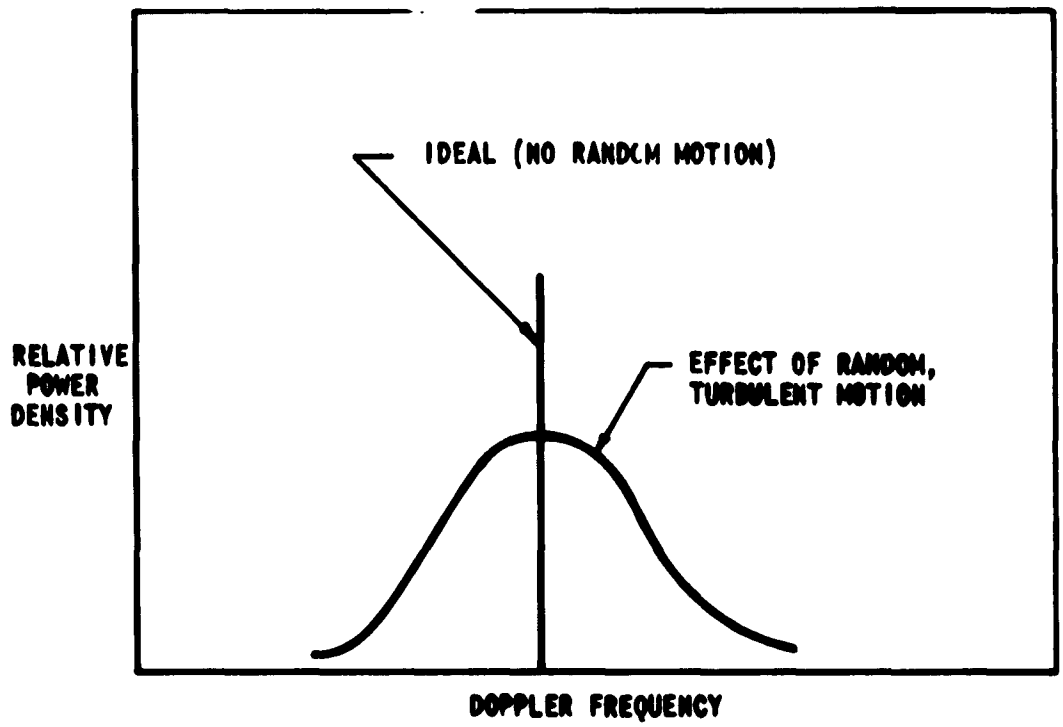

Fig. 3 - Effect of Turbulent Motion on the Doppler Frequency Spectrum

scatter" propagation path. It is believed that the acoustic method will be limited to very short ranges, because of background noise at low frequencies and atmospheric absorption at high frequencies.

There is considerable evidence that radar reflections from turbulence have been detected by existing radar systems. There are, for example, frequent reports of radar "angels" which can be attributed only to turbulent inhomogeneities of the atmosphere. There are reported instances in which such "angels" have been tracked by radar for periods of several minutes. Further evidence in support of this concept may be found in the theories of tropospheric scatter propagation, which are usually based on a mechanism of scattering from an elevated turbulent layer. Radar reflections from periodic disturbances in the atmosphere (see Section II-C) are greatly enhanced at certain ratios of radar to acoustic wavelengths, leading to the belief that radar wavelengths might be varied to provide maximum returns for a given scale of turbulence.

None of this evidence may be regarded as establishing the ability of radar to detect atmospheric turbulence consistently (in the absence of precipitation returns). However, the possibility is so attractive that both the Weather Bureau[5] and the Weather Radar Group under Dr. David Atlas at the Air Force Cambridge Research Laboratories[6] have recently initiated projects to investigate this possibility further. This is also an area of great concern in connection with aircraft warning for avoidance of clear-air turbulence. Considerable progress may be expected toward a satisfactory answer to the question of detectability of atmospheric turbulence in the near future.

One of the most important limitations on the use of atmospheric turbulence for wind velocity measurements will be the attainable range. At present this is difficult to estimate, since no satisfactory theory of radar reflections from atmospheric turbulence exists. Perhaps the best estimate can be obtained from the observations[4] of "angels", which in most cases were within 5,000 yards of the radar. The maximum range to which atmospheric turbulence could be consistently detected under a variety of meteorological conditions must be regarded as at present unknown.

5. Conclusions: The concept of wind measurement by radar determination of mean turbulence velocity is quite attractive due to the use of a natural phenomenon as the remote sensor. Considerably more detailed information will be required, however, regarding the actual characteristics of low-level turbulence, if the feasibility of the concept is to be established analytically. In particular, data will be needed on:

(1) Whether turbulence actually moves with the wind;

(2) The variations of scale for turbulence in the first mile of the atmosphere;

(3) The range of index of refraction variations to be expected;

(4) The range of random, internal velocities of the turbulent cells; and

(5) The probability of having turbulence available under a wide range of atmospheric conditions.

Successful application of this concept would then require that the radar state-of-the-art be advanced to the point where the reliability of back-scatter measurements approached that of present forward-scatter communication systems. If this point is reached, it is believed that statistical processing of the data will enable the resolution of useful, if not exact, velocity information from the ambiguities due to Doppler broadening and the transient buildup and decay of the turbulent cells.

C. Electromagnetic Scattering from Acoustic Waves

1. Method: A technique using electromagnetic scattering from acoustic waves for the remote measurement of low-level wind velocity and temperature profiles has previously been developed and reported[7] by Midwest Research Institute. Through this technique, air velocity is determined by measuring the Doppler frequency shift in an electromagnetic wave that has been reflected from an acoustic wave propagating in the atmosphere. This Doppler frequency corresponds to a velocity that is the sum of the local sound velocity and the component of wind velocity in the direction of acoustic propagation. Since the velocity of sound is a function of air temperature, the Doppler frequency measurement contains both wind and temperature information.

The electromagnetic-acoustic (EMAC) probe consists of a high-intensity directional acoustic source and a Doppler radar system as shown in Fig. 4. To obtain complete wind and temperature information, the volume of interest must be probed from different directions; ordinarily, this will require a separate EMAC probe for each sounding direction. In the most general case, four sounding directions (hence four probes) will be required to determine four quantities; three vector components of the wind velocity and temperature. If certain assumptions can be made, the number of probes can be reduced. These are: if the vertical component of the wind velocity is negligible, then the number of probes needed is reduced to three; and if the air temperature is constant throughout the volume of interest, another probe may be eliminated in favor of a more economical means of temperature measurement.

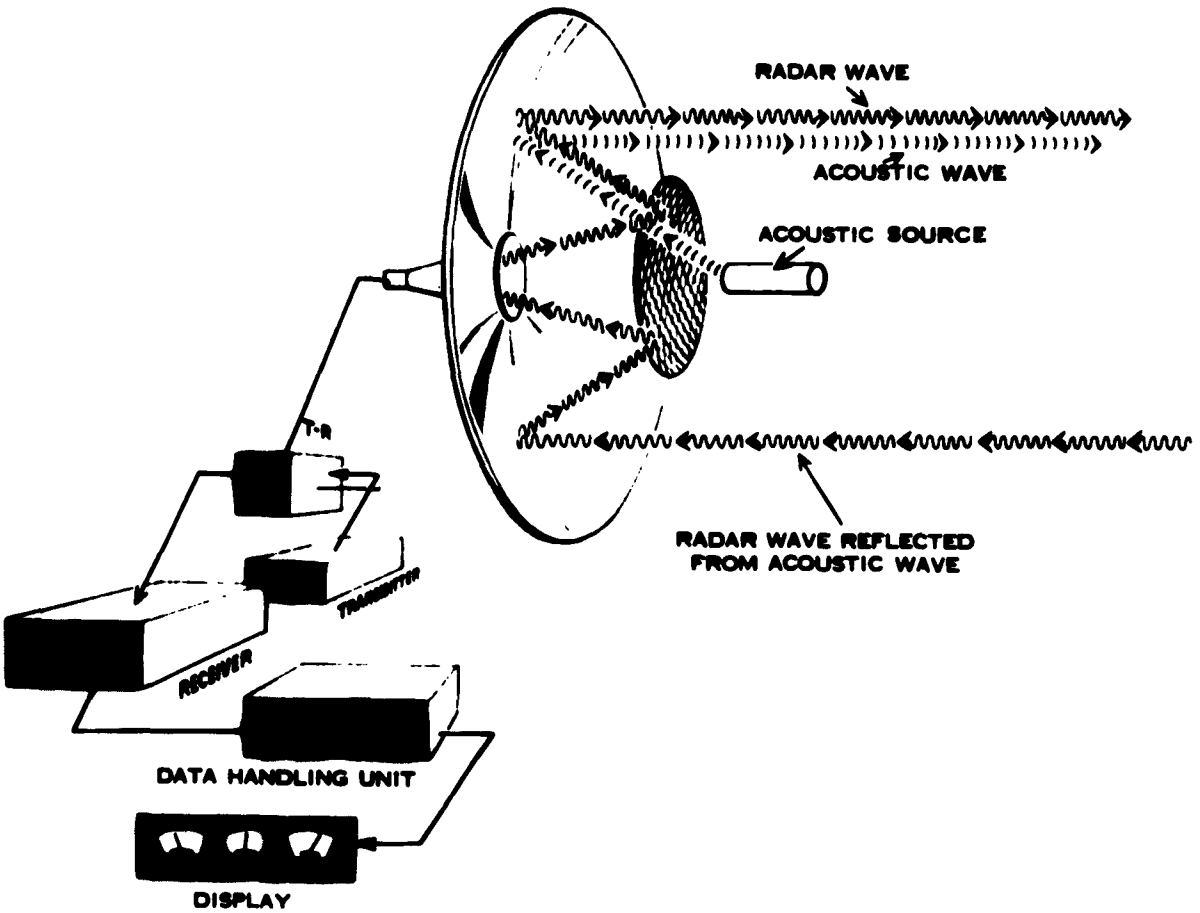

Fig. 4 - EMAC Probe System

In cases where the vertical wind velocity is small, a single EMAC probe can be used to measure temperature profiles only, along a vertical path. Thus, a single probe could be used for sounding low-level temperature inversions in the atmosphere. An accuracy of 1 to 2°F and a height of 1,500 ft. appear to be reasonable performance criteria for this application.

In the reported experimental system, the acoustic signal transmitted is a 6-ms. pulse of 22-kc. frequency. The acoustic intensity is about 140 db. (re 0.0002 dyne/cm^2) at 10 ft. from the source, and the beamwidth is about 5 degrees. The radar system is a 3-w. CW Doppler radar operating at 10,000 mc.; receiver sensitivity is -96 dbm. The acoustic wavelength is 1.5 cm., while that of the radar signal is 3 cm.; this one-to-two wavelength relationship must be maintained to obtain usable reflections.

With this experimental system, radar echoes from the acoustic pulse have been observed out to a distance of about 90 ft. The range is limited chiefly by atmospheric absorption of the acoustic energy which, at 22 kc., exceeds 0.2 db/ft. By operating the system at lower frequencies where absorption is less, the range may be greatly extended. For instance, at 5.5 kc. (6 cm.), the absorption is only 0.06 db/ft and ranges up to 1,500 ft. should be attainable.

A detailed analysis of the EMAC probe wind measuring system has been made[8] and is included in this report as Appendix A. Consequently, enough information about the probe is available to permit good estimates of such performance criteria as range of measurement, accuracy of measurement in speed and direction, resolution, response time, complexity and reliability. Discussions on these performance criteria are given in the following sections.

2. Maximum range of measurement: The maximum operating range of a single EMAC probe is determined by the frequencies employed, transmitter power, receiver sensitivity, condition of the atmosphere, acoustic pulse length and intensity, and the alignment of radar and acoustic wavefronts. The analysis has led to the conclusion that for practical choices of parameters a maximum useful range of 1,500 ft. would be expected for a single probe operating at 2,500 mc. Recent experimental work[9] however indicates that operation may be possible at frequencies as low as 300 mc., with attendant increases in range. The multi-probe arrays required for determining complete wind-vector data will be further limited in range because of scanning requirements; the chief limiting factor here is the loss of accuracy of the multi-probe arrays at the longer ranges. This is due to geometric dilution at the small intersection angles. Examination of the results of the error analysis (Appendix A) shows that the maximum accurate range of a multi-probe array will be comparable to the baseline length available for siting the several probes, and at most will be somewhat less than the maximum range of the individual probes.

3. Accuracy of wind measurement: The probe arrays suitable for determining winds remotely have been designed to provide as outputs the values of two horizontal wind components, which may be regarded as the range and cross-wind components, respectively. The typical accuracy of the measured wind components will be about ± 0.5 mph to ± 1.0 mph; the exact values will vary along the selected profile as the antenna sighting angles vary. Combining these components into the resultant wind vector results in accuracies for the total wind speed of ± 1.0 to ± 1.5 mph.

The accuracy of determination of the wind direction is obviously limited by the accuracy with which the wind vector can be reconstructed from the measured components. If the actual wind speed is only 1 mph, then the errors in the measured components will make accurate determination of the wind direction almost impossible. However, as the wind speed increases the accuracy of the direction determination also increases. For example, referring to Fig. 5, the azimuth error at a wind speed of 10 mph would be about ± 6°. This does not include siting errors and azimuth errors in the alignment of the antenna itself.

4. Three-dimensional resolution of measurement position: For the EMAC probe, the spatial resolution of the wind velocity measurements is a function of many system design parameters. The resolution of a single probe, Fig. 6a, in the radial direction is determined by the spatial length of the acoustic pulse and by the distance the acoustic pulse travelled during the Doppler frequency measurement. An increase in the length of the acoustic pulse is desirable because it increases the radar reflection coefficient of the acoustic wave packet; on the other hand a shorter pulse provides greater spatial resolution. The analysis indicated that a satisfactory compromise can be obtained by using an acoustic pulse length of about 20 to 25 ms. which results in a range resolution of about 25 ft.

In the two dimensions perpendicular to the radial direction, the resolution is governed primarily by the width of the acoustic and radar beams. For a fixed angular beamwidth the resolution distance will increase in proportion to the range. For example, at a range of 250 feet a conical acoustic beamwidth of 6° provides a resolution of about 25 ft., while at a range of 1,000 ft. the resolution would be about 100 ft. In principle, the beamwidth can be reduced to increase the resolution, but problems of increasing antenna size and the difficulty of keeping the acoustic and radar beams aligned will be limiting factors.

When a multi-probe array is used to obtain complete wind vector information, some loss of resolution will result because the probes must examine the volume of interest from different directions.

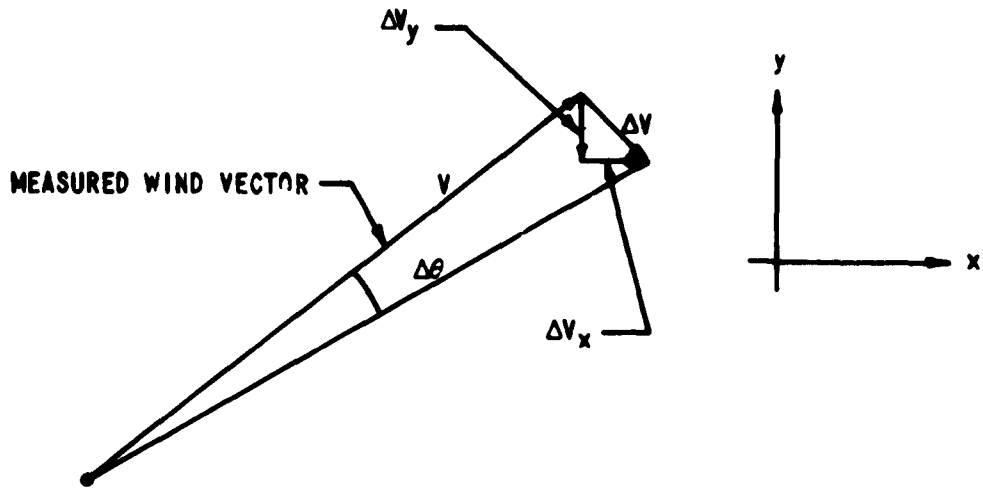

IF $\Delta V_x = 0.7$ MPH

$\Delta V_y = 0.7$ MPH

THEN $\Delta V = 1.0$ MPH

FOR V = 10.0 MPH

$$\Delta\theta \approx \frac{\Delta V}{V} = \frac{1.0 \text{ MPH}}{10.0 \text{ MPH}} = 0.1 \text{ RADIAN}$$

$\Delta\theta \approx 6^\circ$

Fig. 5 - Typical Azimuth Error in Wind Direction for Wind Speed of 10 MPH

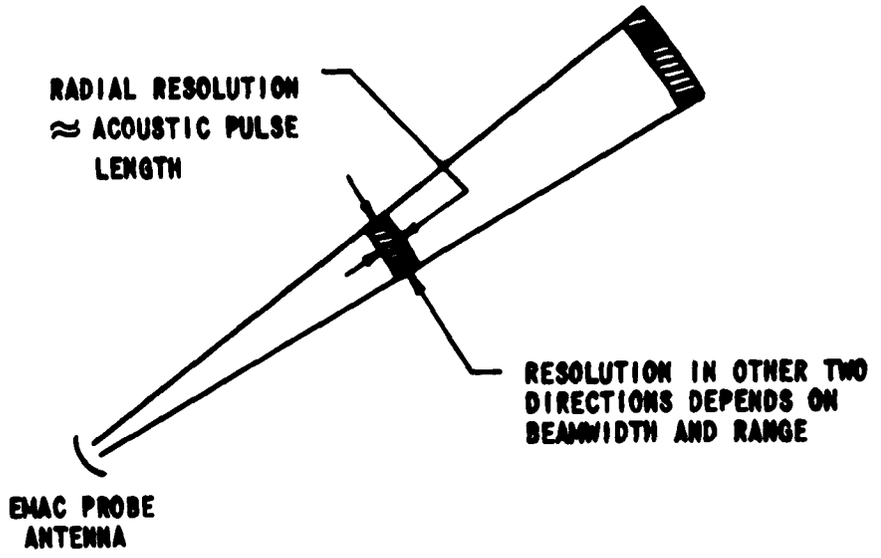

a. Single EMAC Probe

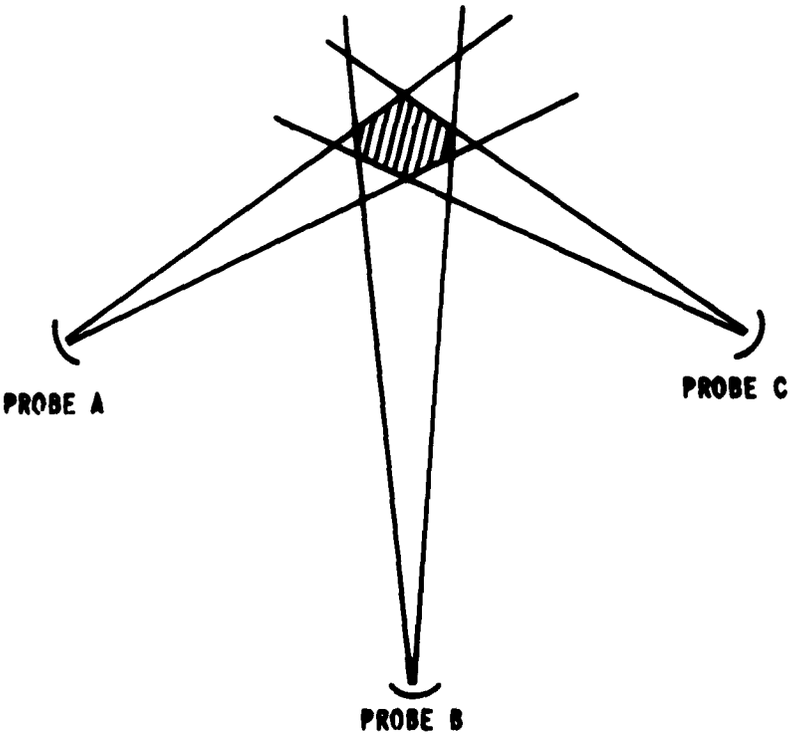

b. Three Probe Array

Fig. 6 - Spatial Resolution of the EMAC Probe System

Figure 6b illustrates a typical situation for a three-probe array; it is evident that the resolution obtainable with a multi-probe array will be comparable to the largest dimension of any of the individual scanning beams at the location being examined.

5. Measurement and display response time: The EMAC probe should actually be characterized by two response times. The first is the time required to make a measurement of the Doppler frequency corresponding to the velocity of the acoustic wave packet at any given location, assuming that the acoustic wave packet has already reached this location. This time will be of the order of a few milliseconds, depending on the particular method of frequency measurement employed and the required accuracy. This response time affords a measure of the ability of the EMAC probe to respond to rapid fluctuations in air velocity or fluctuations of temperature, if provision is made for extracting temperature information from the measurement of sound velocity. The second response time of interest is that required for the scanning of a given profile or a volume of space, which will be determined primarily by the size of the volume of interest and by the propagation time of the acoustic wave. The acoustic signal has a velocity of 1,100 ft/sec, so the time required to scan a radial path with one EMAC probe, out to a distance of 1,100 ft., would be 1 sec. Examination of a larger volume, where several scans in different directions are required, or scanning a single profile with several probes, will require a correspondingly longer time.

As an illustration of this last point, a detailed scanning program suitable for one particular application has previously been worked out.[10] The values of the wind vector at five points out to a maximum range of 300 yd. were determined by a three-probe array. The geometry of the assumed situation is shown in Fig. 7. The required scanning time was found to be about 5 sec. for this particular case.

6. Data presentation form: The experimental versions of the EMAC probe which have been used to date have had only simple forms of data display. These have consisted of oscilloscope presentation of the Doppler signal, and a gated counting circuit used for measurement of the Doppler frequency. In operational versions of the EMAC probe, the display would present either range and crosswind components, or resultant wind speed and direction, or both. The display would probably be in digital form,especially if the equations which must be solved to obtain the wind velocity components from the measured Doppler frequencies are solved by a small digital computer.

Other data which could be displayed include air temperature (actually the so-called "virtual temperature" obtained from the measured sound velocity) and a weighted wind-correction factor suitable for use in fire control or

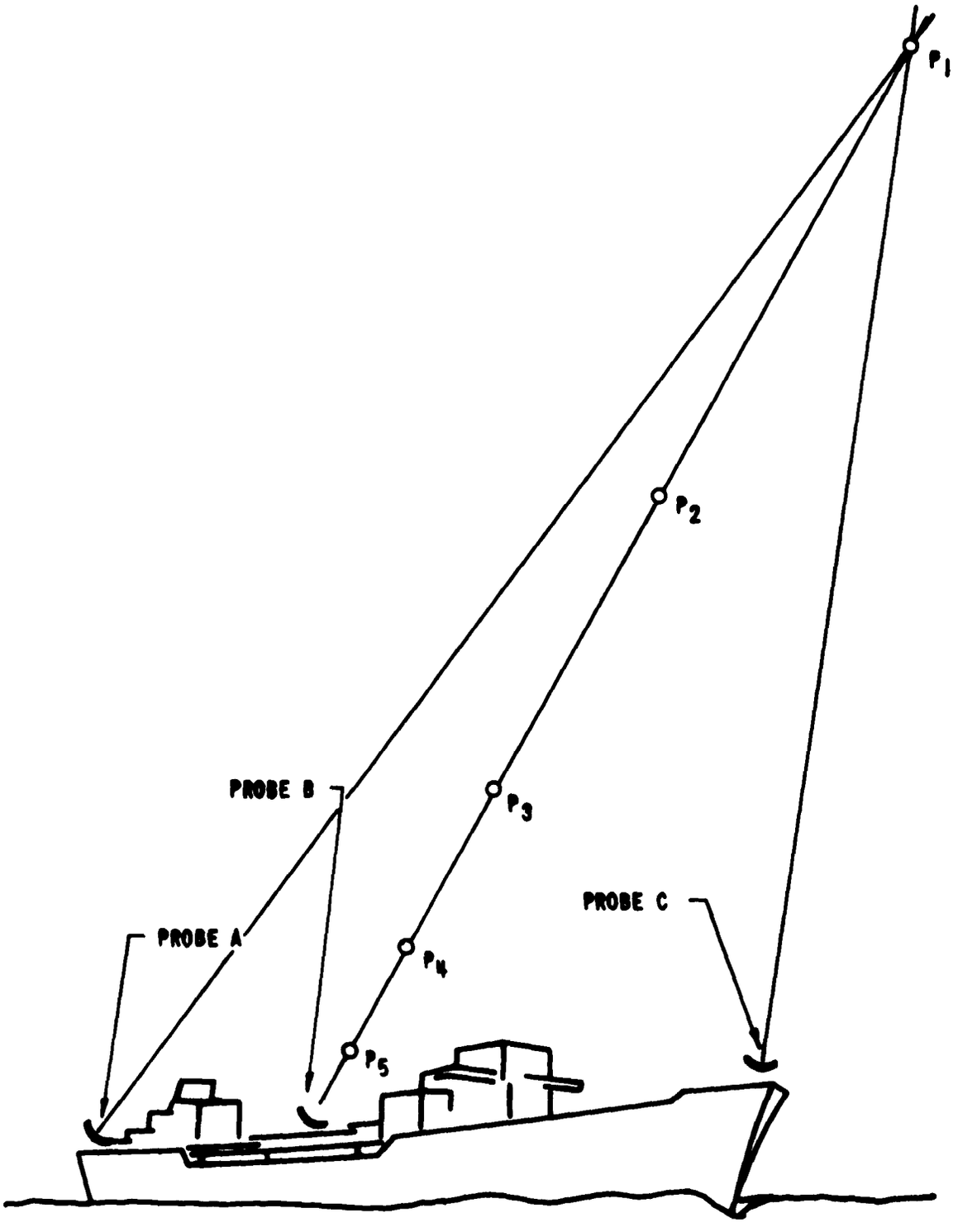

Fig. 7 - A Typical Wind Profile Problem

rocket launching applications. Where the wind-correction factor is desired, it could be calculated by the same computer used to calculate the wind components.

In cases where more complete wind field data are desired, problems of data storage and presentation will be encountered. These problems are not unique to the EMAC probe, but would be encountered in any system intended for measuring a detailed wind field. The data logging equipment at the Cedar Hill tower,[11] which records wind and temperature information at only 12 points, gives some idea of the scope of the problem.

7. Complexity of the required instrumentation: A block diagram of a proposed EMAC probe system is shown in Figs. 8 and 9. Although the complexity of the instrumentation is difficult to estimate from block diagrams, certain conclusions can be drawn. The complexity of the radar portion of the system will be comparable to that of the battlefield surveillance radars now in existence. The acoustic system presents added complexity; however, in the final system design, a fixed acoustic frequency will be used, requiring a very simple acoustic source.

8. Capability for total wind field display: A single EMAC probe can be rotated in azimuth to examine any location within the range of the probe, up to elevation angles of approximately 15 degrees (where the error introduced by neglecting the vertical motion may become significant). However, the single scanning probe gives accurate measurements only when the wind is stratified so that the wind velocity may be considered to be a function of height only. Within the limits imposed by range and elevation coverage, the single-probe system can provide detailed information about the variation of the wind velocity with height.

The ability of the EMAC probe system to display a "simultaneous" wind field is governed by the response time considerations previously discussed. Assuming that the volume of interest is to be scanned in a sequential fashion, a time lapse between measurements at various points in the volume will be inevitable.

9. Reliability: Since only experimental models of the EMAC probe have been built, there is little experience upon which to base judgment of its expected reliability. The radar portion of the probe should compare in reliability to small Doppler radars now in existence. The reliability of the siren acoustic source may present difficulties; moving parts consist of a high-speed siren and a magnetically-operated valve used to pulse the compressed air to the siren. The development of an acoustic source requiring no moving parts would be of considerable advantage.

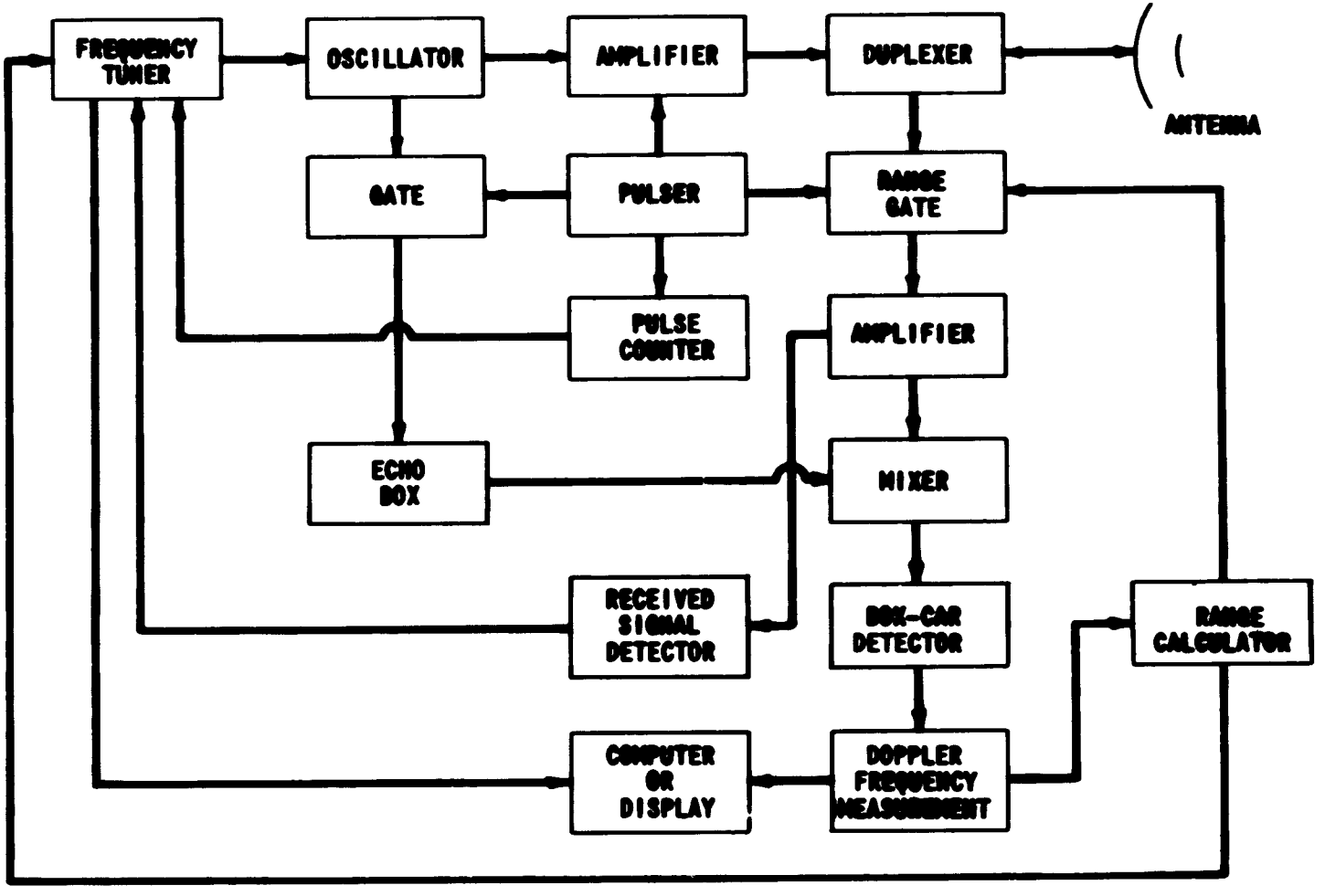

Fig. 8 - Block Diagram of Proposed EMAC Pulse Doppler Radar System

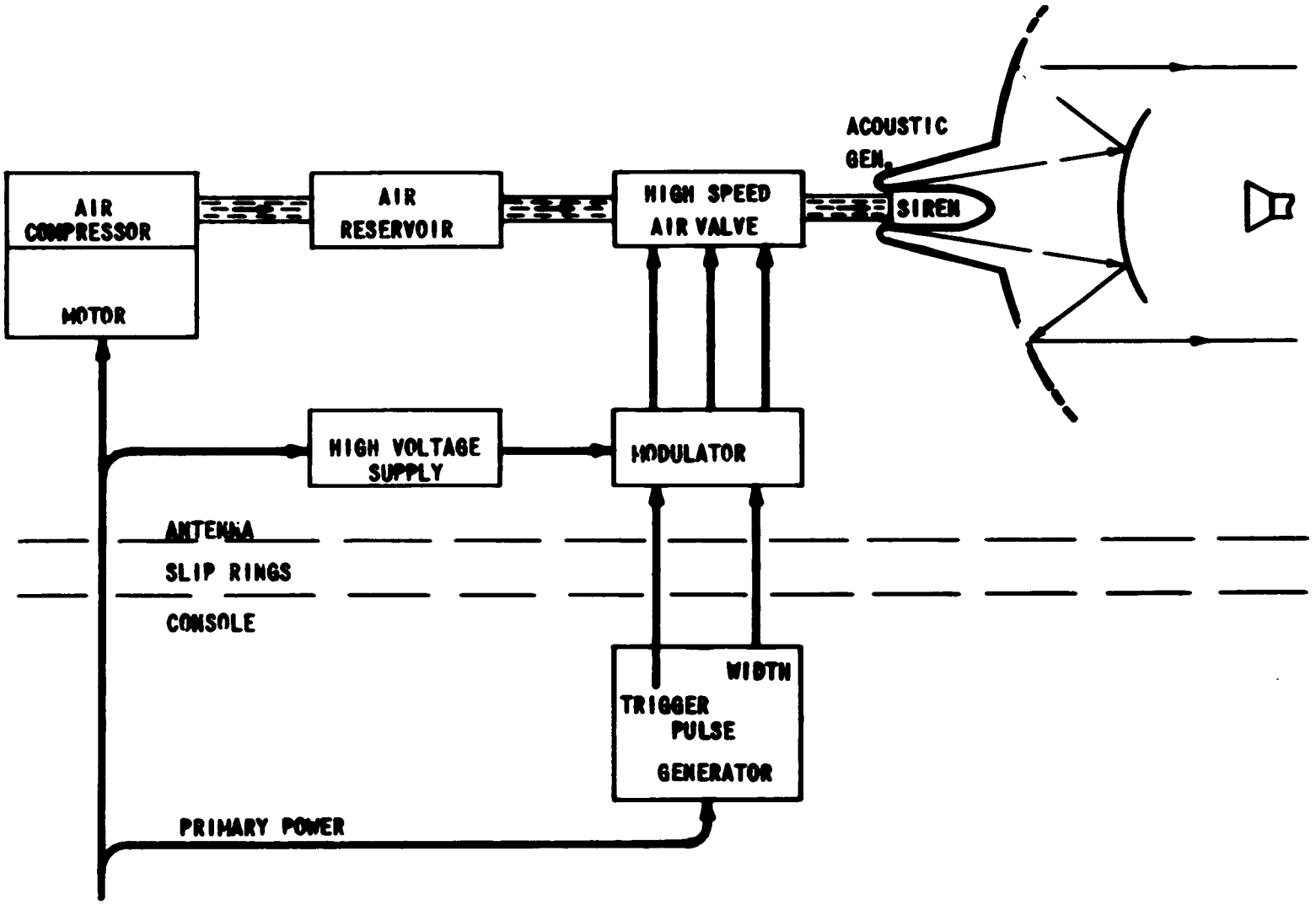

Fig. 9 - Block Diagram of EMAC Probe Acoustic Source

10. Conclusions: The EMAC probe at microwave frequencies appears to be a useful technique for remote wind measurements at ranges up to approximately 1,500 ft. when operating at 2,500 mc. Its extremely fast response to velocity variations and its sensitivity at low velocities make it quite useful for measurement of micrometeorological parameters such as gusts, turbulence, and the detailed thermal structure of the atmosphere.

The resolution of the EMAC probe in time and space depends in a complicated way on several variables such as beamwidths, sensitivity of available receivers, range, and number of probes needed. A single probe has a spatial resolution of 25 ft. or less and a response time of about 50 ms. When an array of probes is used to obtain complete wind and temperature data, the time required to collect and interpret the data from the various soundings will degrade the response time by an order of magnitude. In addition, some loss of spatial resolution will result if the volume of intersection of the several soundings has dimensions greater than 25 ft. The expected accuracies in the measurements will also depend on the particular design, but values of $\pm$ 1 mph in wind velocity and $\pm$ 1°F in temperature are typical.

Its most severe limitation is the maximum range quoted above. This figure is an extension of experimental data at higher frequencies and is believed to be the maximum safe extrapolation of probe characteristics without additional experimental verification. The analysis, when carried to even lower system frequencies, predicts greater usable ranges due to reduced acoustic attenuation, and recent experiments indicate that operation may be possible at frequencies as low as 300 mc. However, additional unknown factors must be investigated before meaningful analytical extrapolations can be made. These factors include attenuation due to turbulent scattering of the acoustic signal, random scattering from turbulence "noise" of the same scale as the acoustic wavelength, and the effects of acoustic beam displacement by the wind at long ranges. Here, as in the preceding method, an increased knowledge of low-level turbulence structure is needed before accurate calculations can be made of expected system performance.

Although this method is the only one of the three that has been demonstrated experimentally, considerable development is needed before a complete long-range wind-field measuring instrument is produced. Further experimental work should be performed to verify the predicted maximum usable ranges for lower frequencies and determine the optimum system parameters for maximum range. In addition, an experimental system could now provide a more precise verification of the EMAC probe theory, permit precise measurements of reflection coefficient and scattering cross-section of the acoustic waves, and provide for the first time an instrument capable of making area, rather than point, measurements of low-level turbulence and wind profiles.

D. Infrared Tracking of an Artificially Heated Bubble

1. Method: This method would use remote means, such as intersecting acoustic, infrared, or microwave beams which could be focused on, and absorbed by a remote volume of air, to raise its temperature above ambient. The heated volume of air, referred to as a bubble, would rise in the atmosphere at a rate dependent on its temperature difference and the local lapse rate. As it rises, its path would be influenced by the local wind field in the same manner as a balloon. Theoretically, the bubble could be tracked by a multiple infrared theodolite system to obtain its position as a function of time, from which the wind profile could be determined.

2. Generation of bubble: The proposed method of bubble generation involved intersecting beams of some form of propagating energy - acoustic, optical, or microwave - capable of being focused on the region to be heated. Such energy transfer and concentration techniques have been used with success where the distances from the transducers to the intersection region are comparable to the spacing between transducers, and to the dimensions of the transducers as shown in Fig. 10. Such a configuration is obviously impractical if ranges of miles or even hundreds of yards are being considered, due to the required size and spacing of radiating elements or transducers. A more usable configuration as shown in Fig. 11 would permit realistic spacing of transducers, but would present additional problems in accurate focusing and aiming to achieve the desired intersection, in poor definition of the intersection point in the radial direction, and in obtaining the required rates of energy input to the bubble.

For the geometry of Fig. 11, if it is assumed, ideally that the beams are perfectly collimated, that they intersect in a common volume, and that no power-sensitive, nonlinear absorption phenomenon, such as ionization, are involved, the power input to the bubble is given by

$$P_{in} = nP_t 10^{-\frac{\alpha d}{10}} \left(1-10^{-\frac{\alpha \ell}{10}}\right) , \qquad (1)$$

where n = the number of transducers,

P_t = the power transmitted by each transducer,

α = the attenuation of the radiation in the atmosphere in db/unit length,

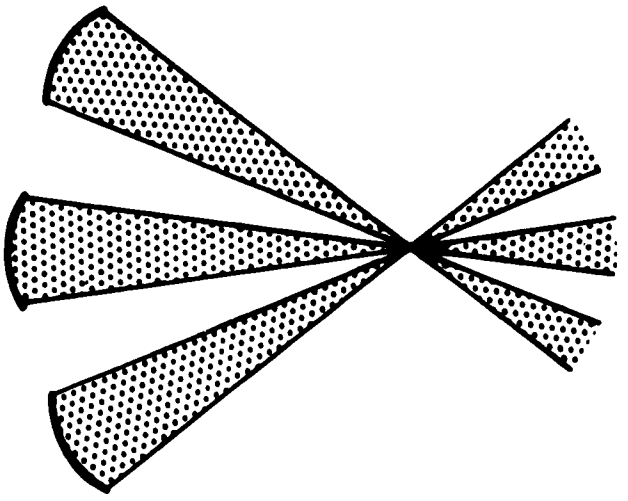

Fig. 10 - Short Range Intersection Geometry

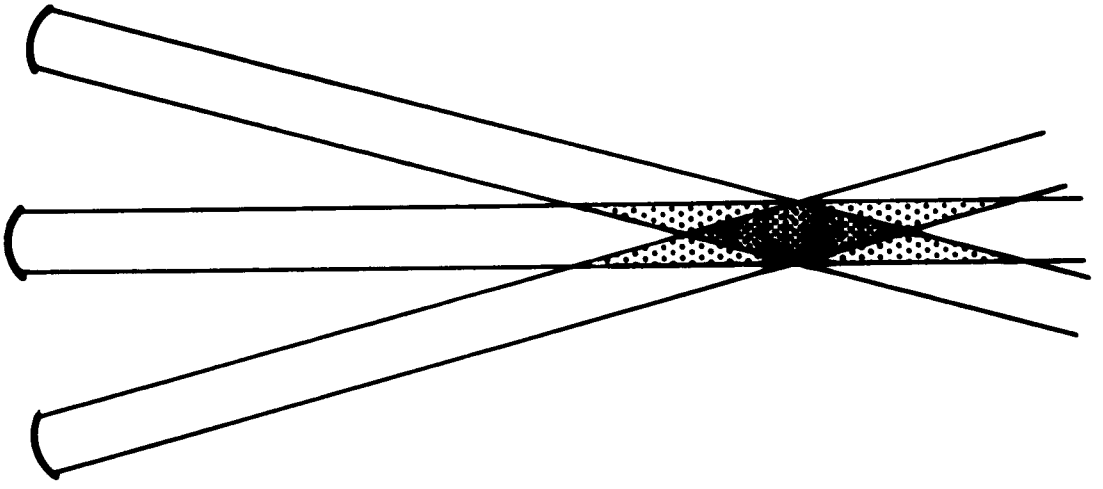

Fig. 11 - Long Range Intersection Geometry

d = the distance to the intersection, and

ℓ = the length of the intersection volume.

Since the absorption is linear in decibels, and d is much greater than ℓ, much more of the available power will be absorbed in the path between bubble and transducer, than in the bubble. As an example, if microwave energy at 24 Gc is used, $\alpha = 0.2$ db/km for air with 1 per cent water vapor. For a 10 meter bubble at 1 km., 4.5 per cent of the power would be absorbed in the path and 0.043 per cent in the bubble. If a frequency such as 190 Gc, with a theoretical $\alpha = 30$ db/km, is chosen to get more absorption in the bubble, the power loss in the path will be 99.9 per cent with only 0.00667 per cent absorbed in the bubble. The intervening paths would obviously be heated much more than the bubble, even if n becomes quite large.

Considering the highly optimistic assumptions concerning this method, it is believed that in the actual case it would be completely impractical. Despite the impracticability of this method of generation, analyses were made of the bubble behavior and detection processes, since it is believed that the information will be of value in situations where other bubble generation schemes may be usable.

3. Analysis of a heated bubble of gas in the atmosphere: The purpose of this analysis is to determine the feasibility of obtaining wind velocity measurements by passive infrared tracking of a gas bubble which is heated and released in the atmosphere. The feasibility depends primarily on the ability of the bubble to maintain sufficient radiance, as it rises through the atmosphere, to be detectable at ground level.

The analyses of the thermodynamic behavior of the bubble and the infrared detection system are detailed in Appendix B and discussed briefly in the following paragraphs.

The model used is a simple one. It is assumed that the bubble rises through the atmosphere adiabatically and that the atmosphere does not mix with the bubble or exert drag or shear forces on it. A consequence of these assumptions is that the model bubble will radiate more power than would be radiated by a bubble in the true atmosphere.

The analysis was made for assumed atmospheres of three different lapse rates: isothermal, 1°C/100 meters, and 2°C/100 meters. For reasons pointed out in Appendix B, a favorable choice of wavelength for detection is 4.1 microns.

A 30 gm. bubble at a height of 1,500 meters, having a temperature of 200°K above the surrounding air, will produce a radiance of about 10^{-5} watts/meter^2-micron at the earth's surface at 4.1 microns. The background noise at the earth's surface is estimated as between 0.1 and 2.0 watts/meter^2-steradian-micron. For a ground-based detector system having a beamwidth of 12 min. of arc, the solid angle of view is 9.5×10^{-6} steradians. Thus, the maximum estimated noise is 1.9×10^{-5} watts/meter^2-micron, that is, the same order of magnitude as the signal. On the basis of the model used, the bubble temperature at ground level would only be a few degrees Kelvin above its temperature at 1,500 meters.

4. Conclusions: An analysis of bubble generation indicates that the original proposal for heating a volume of air with intersecting beams of energy does not appear feasible at distances which are large in terms of transducer size and spacing. This eliminates the "remote" characteristics of the system, as applied to this study. Although the bubble could be generated by other means, such as a distant shell burst or short duration flare, it is believed that presently available techniques such as tracked pilot balloons would offer simpler, more reliable operation.

A parallel analysis of bubble characteristics was made, assuming that the bubble was available in the atmosphere. The thermodynamic model used to represent a hot bubble in the analysis was greatly simplified to make possible a reasonable mathematical treatment. The simplifications, in general, led toward an optimistic view of the bubble's lifetime and behavior. The simple model shows that the assumed bubble could retain its identity as a detectable sensor to a height of 1,500 meters. Additional parameters such as radiation loss, diffusion, turbulent mixing, and shear and drag forces could be included in a much more complex analysis, but the resulting accuracy would suffer from the interaction and uncertainties of the additional model assumptions. It is believed that these parameters will, in general, degrade the bubble configuration, causing it to lose its identity in the first few meters of its travel.

III. CONCLUSIONS

The following conclusions are based on the results of the analyses made during this phase on the three remote wind measurement methods.

A. Scattering From Natural Turbulence

1. Sufficient information on the actual characteristics of low-level turbulence was not available for an adequate analysis to be made of the feasibility of the concept of back-scattering from turbulence.

2. Investigations of this method should be continued because of the advantages of using a natural phenomenon as a sensor.

3. For purposes of further analysis, experimental data should be obtained regarding:

a. The motion of turbulence relative to the wind,

b. The dimensional scale of low-level turbulence,

c. The refractive index variations in low-level turbulence,

d. The random turbulent velocities and their contribution to Doppler broadening, and

e. The probability of occurrence of detectable turbulence.

4. Present radar and acoustic systems lack the required sensitivity for use with this concept.

B. Electromagnetic Scattering From Acoustic Waves

1. This method is feasible for the remote measurement of wind at short ranges.

2. Experimental data are needed to verify existing predictions of capabilities before further theoretical extrapolations can be reliably accomplished.

3. Further improvements in instrumentation are needed to achieve the predicted capabilities and provide data to support existing theory.

4. Experimental investigations should be made to determine how maximum range is affected by such factors as:

a. Attenuation due to turbulent scattering of the acoustic wave,

b. Radar scattering from turbulence of the same scale as the acoustic wavelength, and

c. Acoustic beam displacement by the wind.

C. Infrared Tracking of an Artificially Heated Bubble

The generation of a well defined heated region by intersecting beams of energy is not feasible for system geometries applicable to this method.

IV. PROGRAM FOR NEXT PHASE

The objective of the next phase is to design experiments capable of verifying the assumptions and results of the analyses performed in this phase, and to consider the instrumentation required to conduct the experiments designed. Experiments will be designed to determine the parameters listed below.

A. Scattering From Natural Turbulence

1. The motion of turbulence relative to the wind.

2. The dimensional scale of low-level turbulence.

3. The refractive index variations in low-level turbulence.

4. The random turbulent velocities and their contribution to Doppler broadening.

5. The probability of occurrence of detectable turbulence.

B. Electromagnetic Scattering From Acoustic Waves

1. Maximum range as a function of system frequencies.

2. Reflection coefficient and scattering cross section of acoustic waves for verification of theory and extension of analysis.

3. Attenuation due to turbulent scattering of the acoustic wave.

4. Acoustic beam displacement by wind and turbulence.

5. Radar scattering from turbulence of the same scale as the acoustic wavelength.

C. Infrared Tracking of an Artificially Heated Bubble

No experimental design is recommended for this method.

V. PERSONNEL

The following personnel have contributed to the project for the number of man-hours listed.

Harold L. Stout, Assistant Director, Engineering Division - 32 man-hours.

Paul C. Constant, Jr., Head, Electronics Engineering Section - 48 man-hours.

Richard W. Fetter, Senior Engineer - 400 man-hours.

Paul L. Smith, Jr., Senior Engineer - 222 man-hours.

George E. Chambers, Assistant Engineer - 32 man-hours.

B. L. Jones, Associate Engineer, 100 man-hours, B.S. in E.E., 1947, University of Kansas, Graduate Studies in Physics, 1947-1948, University of Kansas. Mr. Jones' special fields are transmission lines and electromagnetic radiation and propagation. His technical experience includes work on vibration suppression, automation, and propagation phenomena with regard to random and induced disturbances in the atmosphere.

Harold F. Schick, Senior Engineer, 288 man-hours, B.S. in Electrical Engineering, 1954, Cooper Union; M.S. in Electrical Engineering, 1961, University of Arizona. Mr. Schick has thirteen years' experience in the design and analysis of electronic systems. The past seven years he has been largely concerned with air-borne systems having stringent requirements with regard to reliability, bandwidth utilization, minimum noise, and high energy density performance. A significant phase of the design and analysis has entailed evaluation and optimization techniques.

Robert M. Stewart, Jr., Consultant, 56 man-hours, B.S. in Electrical Engineering, 1945, and Ph.D. in Physics, 1954, Iowa State College. Mr. Stewart's special fields are thermal and mechanical atmospheric turbulence and digital and analog computer solutions of meteorological problems. His technical experience includes teaching electromagnetic wave theory.

BIBLIOGRAPHY

1. Papa, R. J., "Atmospheric Turbulence," Geophysics Corp. of America, Scientific Report No. 7, for Air Force Cambridge Research Laboratories AD 257-842, April, 1961.

2. Richards, E. J., and J. E. Ff. Williams, "Some Recent Developments in Jet Noise Research," University of Southampton, Department of Aeronautics and Astronautics, Report No. 118, August, 1959. See also Bull, M. K., "Instrumentation for and Preliminary Measurements of Space - Time Correlations and Convection Velocities..." University of Southampton, Department of Aeronautics and Astronautics, Report No. 149, August, 1960.

3. Bricourt, Pierre, et al., "Ultrasonic Technique for the Determination of Wind Velocity Measurements," Emerson Research Laboratories, 1140 East-West Highway, Silver Springs, Maryland, Final Report No. FR-5122, Contract No. NObs-84140 to Bureau of Ships, Department of the Navy; 3 April 1961.

4. Tillman, R. Q., et al., "A Study of Clear-Air Angels by the Use of Horizontal and Vertical Trajectories," Proc. Ninth Weather Radar Conference, Kansas City, Missouri, pp. 241-246, 23-26 October 1961.

5. Stewart, P. G., "Radar in Turbulence Research," ibid., pp. 206-211.

6. First Phase Report, p. 44.

7. Smith, P. L., Jr., and R. W. Fetter, "Remote Measurement of Wind Velocity by the Electromagnetic - Acoustic Probe. I: System Analysis. II: Experimental System," Conference Proceedings, Fifth National Convention on Military Electronics, Washington, D. C., pp. 48-59, June, 1961.

8. Fetter, R. W., P. L. Smith, Jr. and V. Klein, "Design Concept Study for a Wind Profile Instrument," Final Report, Contract No. DA-23-072-506-ORD-11 to U. S. Army Rocket and Guided Missile Agency from Midwest Research Institute, November, 1960.

9. Private communication from Mr. R. W. Sutton, The Boeing Co., Seattle, Wash.

10. Fetter, R. W. and P. L. Smith, Jr., "A Study of Possible Applications of the EMAC Probe Aboard Navy Ships," Final Report, Contract No. NOw 61-0720-d to Bureau of Weapons, Department of the Navy from Midwest Research Institute, pp. 14-20, October, 1961.

BIBLIOGRAPHY (Concluded)

11. Stevens, D. W., "Cedar Hill Meteorological Research Facility," Instrumentation for Geophysics and Astrophysics, No. 18, GRD, Air Force Cambridge Research Laboratories, ASTIA No. AD 263 847, June, 1961.

APPENDIX A

ANALYSIS OF ELECTROMAGNETIC-ACOUSTIC (EMAC) PROBE

This analytical treatment of the EMAC probe was originally performed on contract No. DA-23-072-506-ORD-11, with the Army Rocket and Guided Missile Agency and is included here to make available the mathematical procedures and results as they apply to the present analysis.

I. RANGE PERFORMANCE OF THE EMAC SYSTEM

The range performance of the EMAC probe for remote measurement of wind velocities is limited chiefly by the decrease in the reflection coefficient of the acoustic disturbance with increasing distance from the source. This decrease is the result of two factors: the divergence of the acoustic wave and the absorption and scattering by the atmosphere of some of the acoustic energy. Since the absorption increases with the acoustic frequency, the use of as low a frequency as is compatible with other requirements of the system is indicated.

A. Calculation of Received Power

To obtain a quantitative estimate of the ultimate range of the EMAC system, consider a system in which the acoustic and radar sources are located at the same point. This arrangement is advantageous because the spherical acoustic wavefronts act like concave mirrors in focusing the reflected electromagnetic energy back toward the source.

1. Reflected power: The microwave power density impinging on the acoustic wave train at a distance r from the source is

$$P_i = \frac{P_t G}{4\pi r^2} \qquad \text{(A-1)}$$

The power reflection coefficient ρ^2 of the acoustic wave train has been computed previously.[1] The reflected power per unit area of the acoustic wavefront will be

$$P_r = P_i \times \rho^2 = \frac{P_t G}{4\pi r^2} \rho^2 . \qquad \text{(A-2)}$$

The total reflected power is the product of this reflected power density and the area of the acoustic disturbance illuminated by the radar signal. Because of the divergence of both the acoustic and radar beams, the illuminated area will increase in proportion to the square of the distance. The illuminated area, of course, never can be greater than $\frac{4\pi r^2}{G}$, and, in general, will be only some fraction f of this quantity. Then the total reflected power will be

$$P_{tr} = \frac{P_t G}{4\pi r^2} \rho^2 \frac{4\pi r^2 f}{G}$$

$$= P_t \rho^2 f \ . \qquad \text{(A-3)}$$

The value of f depends on the matching of the geometry of the acoustic and radar beams. For best results, the beam widths should be made equal -- this will insure that most of the radar power is concentrated where the acoustic beam is most intense, hence, where the reflection coefficient is greatest.

2. Received power: Because of the focusing action of the acoustic wavefronts, a rather large fraction g of the total reflected power will be returned to the radar receiver. The total received power will be

$$P_r = P_t \rho^2 f g \ . \qquad \text{(A-4)}$$

The product fg is a measure of beam and wavefront alignment.

The dependence of the power reflection coefficient on the acoustic signal may be expressed as[1]

$$\rho^2 = K \left(\frac{\Delta c}{c}\right)^2 \ , \qquad \text{(A-5)}$$

where the parameter K has the value 61.6 for an acoustic signal 10 cycles long and is proportional to the square of the number of cycles in the acoustic signal. The relationship of the quantity $\left(\frac{\Delta c}{c}\right)$ to the intensity of the acoustic signal is[2]

$$\frac{\Delta\epsilon}{\epsilon} = 1.2 \times 10^{-13} \times \sqrt{\frac{I}{I_o}} \quad , \tag{A-6}$$

Using these values, the reflection coefficient of the acoustic signal is

$$\rho^2 = 1.44K \times 10^{-26} \times \left(\frac{I}{I_o}\right) \quad . \tag{A-7}$$

The acoustic intensity decreases with distance from the source according to the equation

$$I = I_1 \left(\frac{r_1}{r}\right)^2 10^{-\frac{\alpha}{10}(r-r_1)} \quad . \tag{A-8}$$

The power reflection coefficient is therefore

$$\rho^2 = 1.44K \left(\frac{r_1}{r}\right)^2 \times 10^{-26} \times \frac{I_1}{I_o} \times 10^{-\frac{\alpha}{10}(r-r_1)} \quad . \tag{A-9}$$

For this value of reflection coefficient, the power received at the antenna is

$$P_r = P_t \frac{r_1^2 (1.44)K \times 10^{-26} \times I_1 \times 10^{-\frac{\alpha}{10}(r-r_1)}}{r^2 I_o} \text{ fg}$$

or

$$\frac{P_r}{P_t} = 1.44 \times 10^{-26} \frac{r_1^2 K \times I_1 \times 10^{-\frac{\alpha}{10}(r-r_1)}}{r^2 I_o} \text{ fg} \quad . \tag{A-10}$$

B. Typical Values of Transmission Loss

1. Values of the parameters: An optimistic estimate of the received power is obtained from the following values:

$$(fg) = 1; \; I_1 = 140 \text{ decibels at } r_1 = 10 \text{ ft.}$$

(this value of I_1 has been attained by an experimental siren). The value of K depends upon the number of cycles employed in the acoustic signal which, in turn, is limited by the range resolution requirement. For purposes of the subsequent calculation, an acoustic wave train length of 25 ft. will be used. It is believed that this length represents the maximum allowable range uncertainty, while still producing usable reflections. At a frequency of 22 kc. (wavelength 1.5 cm.) a 25-ft. long acoustic signal will consist of 500 cycles in the direction or propagation. The corresponding numbers of cycles in 25 ft. for other frequencies are indicated in Table A-I.

TABLE A-I

VALUES OF THE PARAMETER K FOR SEVERAL ACOUSTIC FREQUENCIES

Acoustic Frequency (kc.)	Acoustic Wavelength (cm.)	No. of Cycles in 25 Ft.	K
22	1.5	500	154,000
11	3	250	38,500
7.33	4.5	166	17,000
5.5	6	125	10,000

The value of the absorption constant α depends in a rather complicated way upon frequency and relative humidity.[3] Values for the absorption constant at 30, 50 and 70 per cent relative humidity are plotted as a function of frequency in Fig. A-1; the data were taken from Knudsen's curves.[3] At 50 per cent relative humidity the variation of α with frequency is approximately linear, with the equation

$$\alpha = (0.0107\ f_a - 0.02)\ \text{db/ft} \qquad \text{(A-11)}$$

representing the values for frequencies above 4 kc. Note that for other relative humidities the dependence of α on frequency is not linear; for lower relative humidities the absorption will be higher than at 50 per cent R.H., and for higher humidities it will be lower.

Knudsen's data extend only to 10 kc. in frequency; the values listed below for the absorption constant α at higher frequencies have been obtained by extrapolating the linear relationship of (A-11):

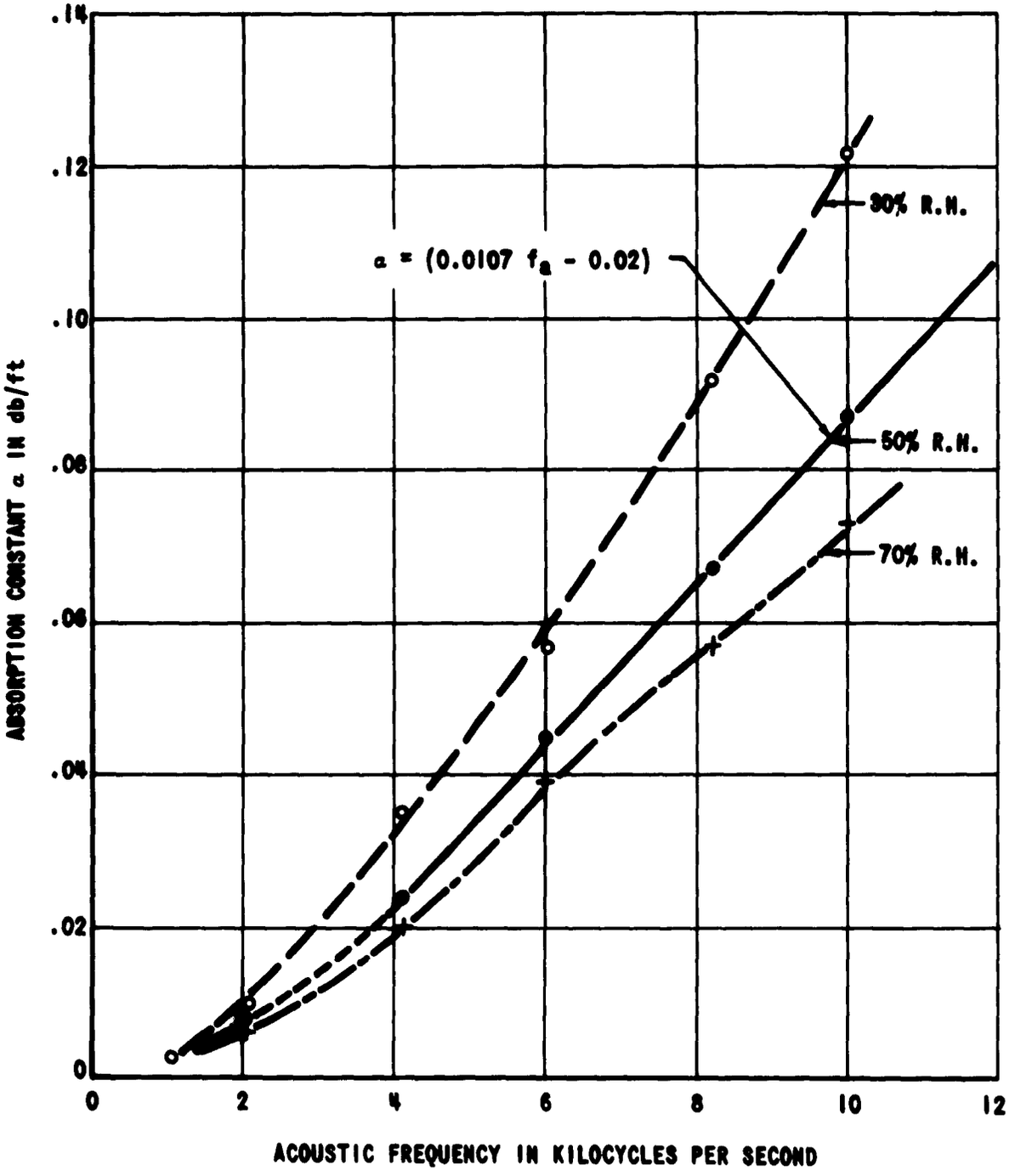

Fig. A-1 - Absorption Constant for an Acoustic Wave in Air

α = 0.22 db/ft at 22 kc., 50 per cent R.H.;

α = 0.10 db/ft at 11 kc., 50 per cent R.H.;

α = 0.06 db/ft at 7.3 kc., 50 per cent R.H.;

α = 0.04 db/ft at 5.5 kc.; 50 per cent R.H. (A-12)

A plot of acoustic intensity vs. range for these frequencies is shown in Fig. A-2.

2. Values of transmission loss: Using these values in (A-10), the following equations for received power at the various acoustic frequencies are obtained:

$$\left.\frac{P_r}{P_t}\right]_{22\ kc} = 2.21 \times 10^{-5}\ \frac{10^{-0.022(r-10)}}{r^2}\ ;$$

$$\left.\frac{P_r}{P_t}\right]_{11\ kc} = 5.55 \times 10^{-6}\ \frac{10^{-0.01(r-10)}}{r^2}\ ;$$

$$\left.\frac{P_r}{P_t}\right]_{7.3\ kc} = 2.45 \times 10^{-6}\ \frac{10^{-0.006(r-10)}}{r^2}$$

$$\left.\frac{P_r}{P_t}\right]_{5.5\ kc} = 1.44 \times 10^{-6}\ \frac{10^{-0.004(r-10)}}{r^2} \qquad \text{(A-13)}$$

The above ratios, in decibels of transmission loss where

$$db = -10 \log \frac{P_r}{P_t}\ , \qquad \text{(A-14)}$$

are plotted as a function of range in Fig. A-3. Assuming a rather idealized receiver sensitivity of -135 dbm, values of the maximum usable transmission loss for transmitted powers of 10 watts, 100 watts and 1 kw. have been indicated by the horizontal lines on the figure. The meaning of these curves

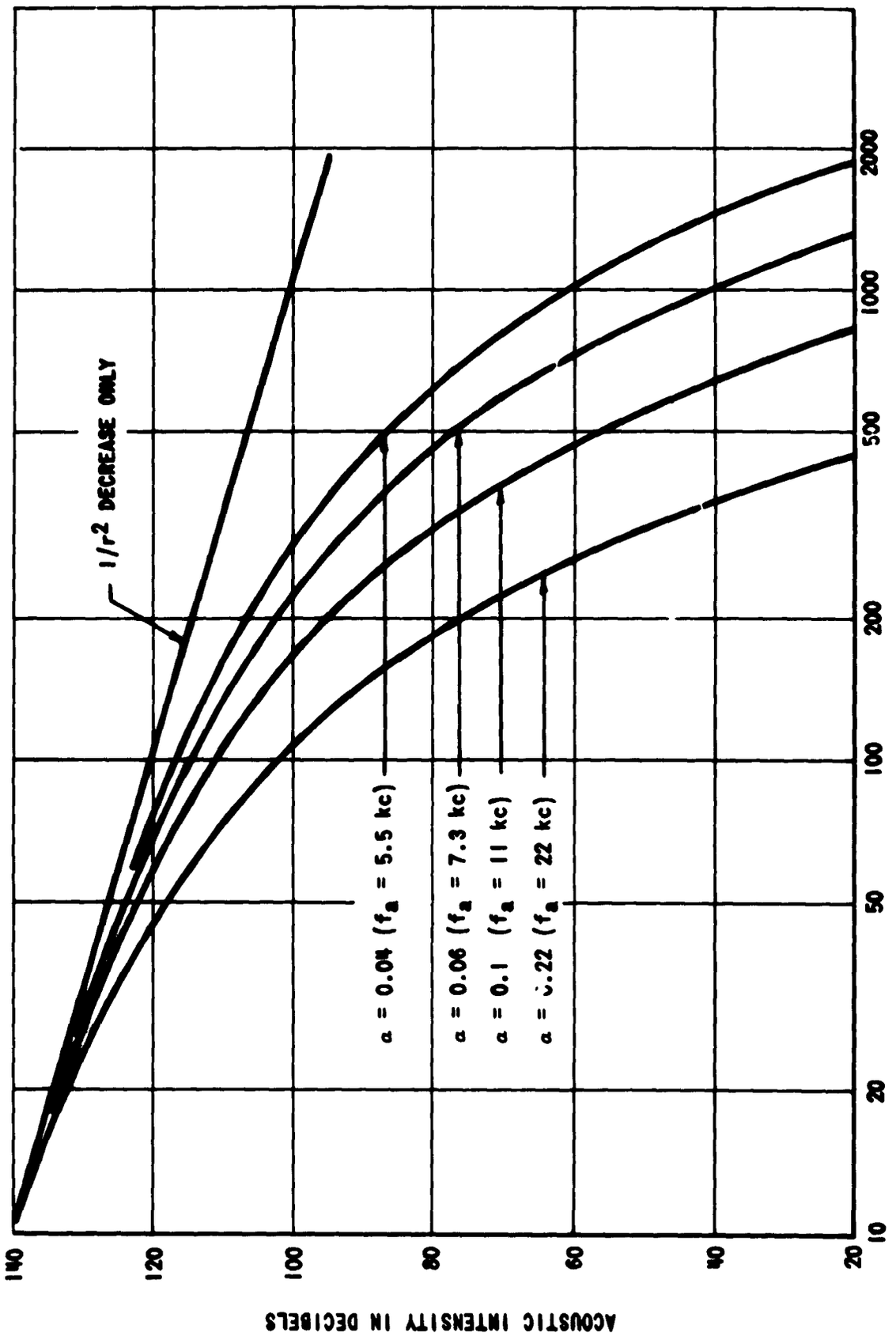

Fig. A-2 - Effect of Atmospheric Absorption on Acoustic Intensity

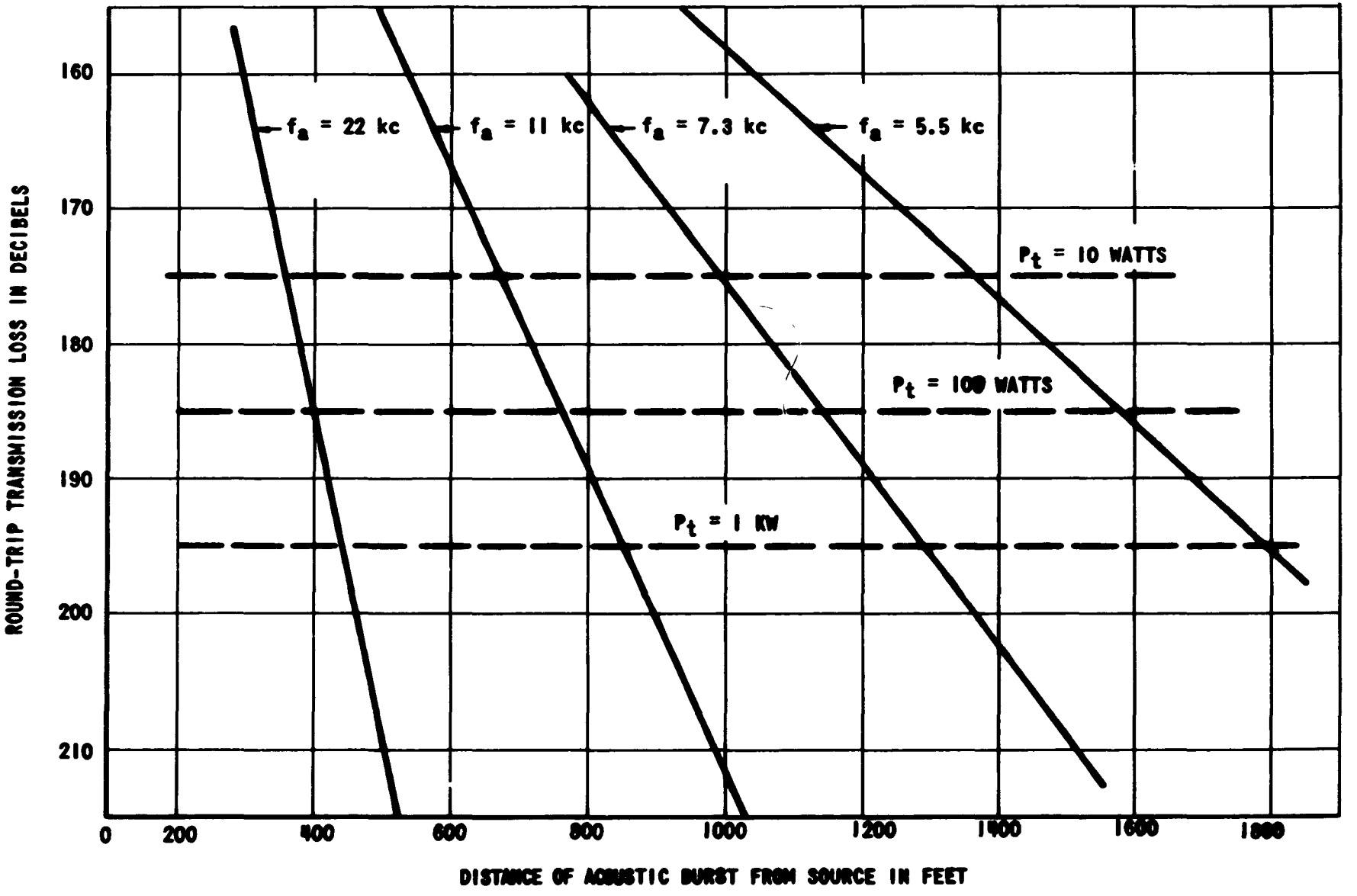

Fig. A-3 - Round Trip Transmission Loss vs. Distance for Ideal System

will be clearer from the following example: suppose a transmitter power of 100 watts is used with a receiver of sensitivity - 135 dbm. Then for various choices of acoustic frequency (and the corresponding radar frequency determined from $\lambda_e = 2\lambda_a$) the maximum range will be as given in Table A-II.

TABLE A-II

MAXIMUM RANGE OF EMAC SYSTEM FOR VARIOUS FREQUENCIES

Acoustic Frequency (kc.)	Radar Frequency (mc.)	Maximum Range (ft.)
22	10,000	400
11	5,000	760
7.3	3,300	1,140
5.5	2,500	1,570

C. Maximum Receiver Sensitivity

The available noise power at the input to the receiver will be of the order of 4×10^{-15} watts per megacycle of receiver bandwidth.[4] If a receiver with a noise figure of 3 db. is used, the equivalent noise power input to the receiver will be 8×10^{-15} watts per megacycle of bandwidth. The required bandwidth depends on the amount of Doppler shift which will be contributed by the wind velocity; for maximum winds of 75 mph, the required bandwidth will be roughly 150 times the Doppler shift in cycles per second per mile per hour of wind velocity. Typical values of receiver bandwidth, equivalent noise power input and maximum attainable receiver sensitivity for a receiver capable of detecting a signal equal in power to its equivalent input noise power, are shown in Table A-III.

D. Scattering Due to Turbulence in the Atmosphere

An additional factor which may affect the probe performance at longer ranges is the scattering of the acoustic signal by atmospheric turbulence. This scattering will be seen by the system as increased attenuation of the acoustic wave.[5] The amount of scattering attenuation depends upon both the scale of the turbulent eddies and the magnitude of the fluctuations in the properties of the atmosphere. Because of the lack of information on these effects, it is difficult to establish a quantitative estimate of the attenuation constant to be expected.

TABLE A-III

MAXIMUM ATTAINABLE SENSITIVITY FOR RECEIVER WITH 3 DB. NOISE FIGURE

Acoustic Frequency (kc.)	Microwave Frequency (mc.)	Doppler Shift (cps/mph)	Approximate Bandwidth Required (kc.)	Equivalent Noise Power Input (x 10^{-17} watts)	Maximum Receiver Sensitivity (dbm)
22	10,000	30	55	4	-134
11	5,000	15	2.5	2	-137
7.3	3,300	10	2	1.6	-138
5.5	2,500	7.5	1.5	1.2	-139

However, analysis shows[5] that it is probable that the attenuation of the acoustic signal due to scattering could exceed that due to atmospheric absorption. The range performance of the EMAC probe would be reduced by this additional attenuation, but no convenient quantitative evaluation of the reduction is possible.

The attenuation constant due to scattering is, however, known to be proportional to the square of the acoustic frequency.[5] The use of a lower acoustic frequency will therefore reduce the attenuation from this cause as well as from absorption.

E. Experimental Verification

Experimental measurements were made on the basic EMAC probe to verify the theoretically derived equation for the function, P_r/P_t, for the system, based upon an assumed value for the factor fg in (A-10). For reference, the basic equation is:

$$\frac{P_r}{P_t} = 1.44 \times 10^{-26} \frac{r_1^2 \, K \times I_1 \times 10^{-\frac{\alpha}{10}(r-r_1)}}{r^2 \, I_o} fg \, , \qquad \text{(A-10)}$$

where the parameters and their measured values are:

P_r = power received at antenna = -96 dbm (receiver sensitivity);

P_t = power transmitted = +34.8 dbm (3 watts);

I_o = reference acoustic intensity (defined) 10^{-16} watts/cm^2 = 0 db.;

I_1 = acoustic intensity at a range r_1 = 140 db.;

$\frac{I_1}{I_o}$ = 140 db. or 10^{14};

r_1 = range at which I_1 is measured = 10 ft.;

r = maximum range of detection = 90 ft.; and

α = the acoustic absorption constant = 0.22 db/ft for 22 kc.

The parameters which were not measured are:

f = the fraction of the acoustically disturbed area which is illuminated by microwaves;

g = the fraction of the reflected energy which is intercepted by the receiving antenna; and

K = derived constant determined by length of acoustic wave train = 10^4 for 132 wavelengths in a 6-ms. wave train.

The measurement of f, g, and K for the experimental system was beyond the scope of this program, so complete verification of (A-10) was not possible. To complete the calculation, the derived value of $K = 10^4$ and an initial assumption of $fg = 1$ were used. The assumption for fg implies that the system is ideal, that is, all microwave energy interacts with the acoustic disturbance and all energy that is reflected is focused on the receiving antenna. This optimistic assumption gives a predicted maximum range of 142 ft. When compared with the measured value of 90 ft., a discrepancy of 16 db. is indicated in the over-all transmission loss. This is shown in Fig. A-4, which is a plot of P_r/P_t in decibels as a function of range for the experimental system. A more realistic estimate of fg was obtained by assuming that all the reflected energy was returned from interaction within the 5°, half-power beam width of the main lobe of each antenna and that the acoustic wave front geometry fell half way between the spherical shape produced by a point source and the plane waves produced by a perfectly focused reflector. From these considerations, a value of $fg = 1/30$ was obtained. While this number is not exact, it is much more realistic than the first assumption and leads to a predicted maximum range of 93 ft., or a discrepancy of 1.5 db. in transmission loss. This agreement is sufficiently good to justify using the theory to predict the performance of systems operating at other frequencies and power levels.

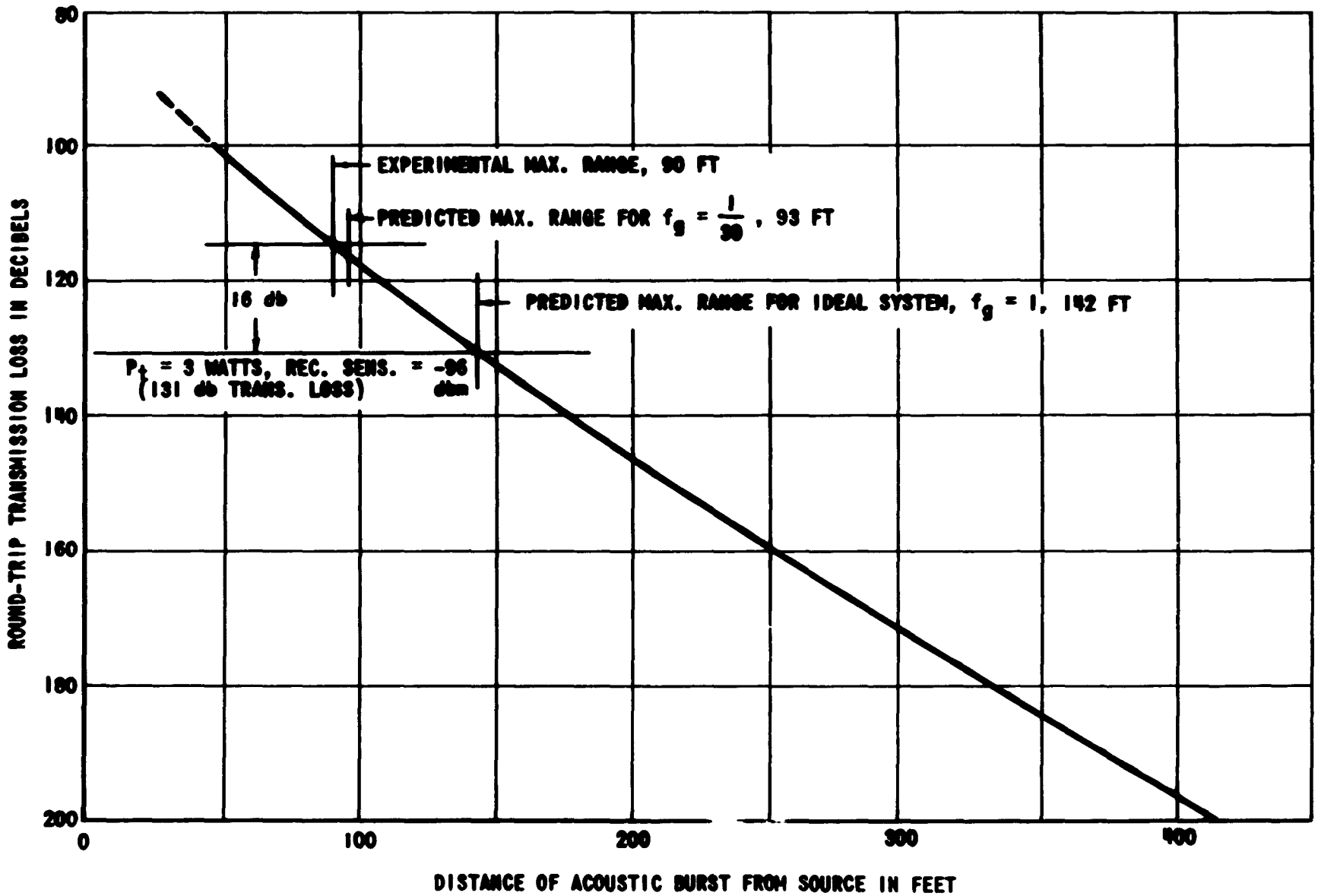

Fig. A-4 - Round Trip Transmission Loss vs. Distance for Experimental System

To obtain complete correlation between the theoretical and experimental system characteristics, accurate measurements of f, g, and K should be made, preferably at lower system frequencies where much greater ranges are predicted and the system performance should be more sensitive to parameter variations.

... SYSTEM CONFIGURATIONS FOR OBTAINING WIND VELOCITY PROFILES

A. Requirements of the System

The EMAC probe measures the vector sum of the velocity of propagation of the acoustic signal through air and the component of wind velocity in the direction of propagation. Since the wind velocity may be represented as a vector with three spatial components, the system will be required to gather four independent pieces of data from which the four quantities v_s, W_x, W_y and W_z may be determined. In general, these four pieces of data will be obtained from four soundings made by an EMAC probe or probes in different directions.

In particular situations only three such soundings may be required. This would be the case if only horizontal components are desired, or if it can be assumed that the vertical component of the wind is much smaller than the other two components. In the usual meteorological reports the vertical component is not even considered. If the vertical component is neglected, only three soundings are required, since only three of the unknowns remain.

B. System Using One Steerable EMAC Probe

For the case of low elevation angles, the two horizontal components of the wind velocity vector can be obtained by taking three soundings in different directions with a single EMAC probe operating from a fixed site at the launching point. The directions of the soundings are shown schematically in Fig. A-5.

1. Method of obtaining wind velocity components: If the wind vector is

$$\bar{W} = W_x \bar{i} + W_y \bar{j} + W_z \bar{k} , \qquad \text{(A-15)}$$

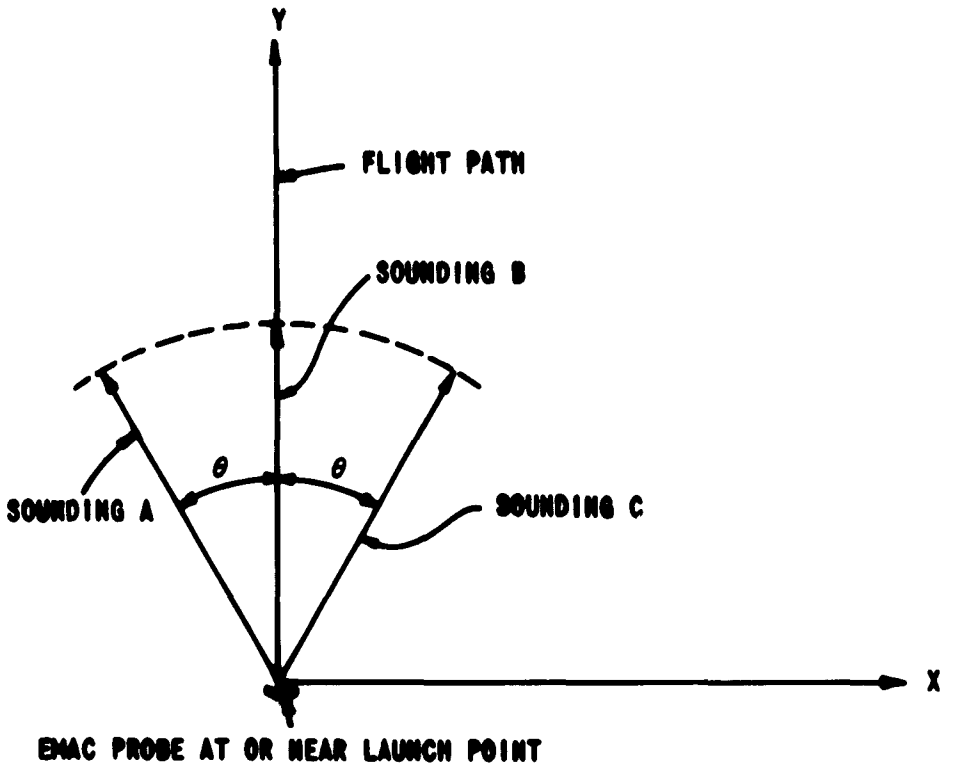

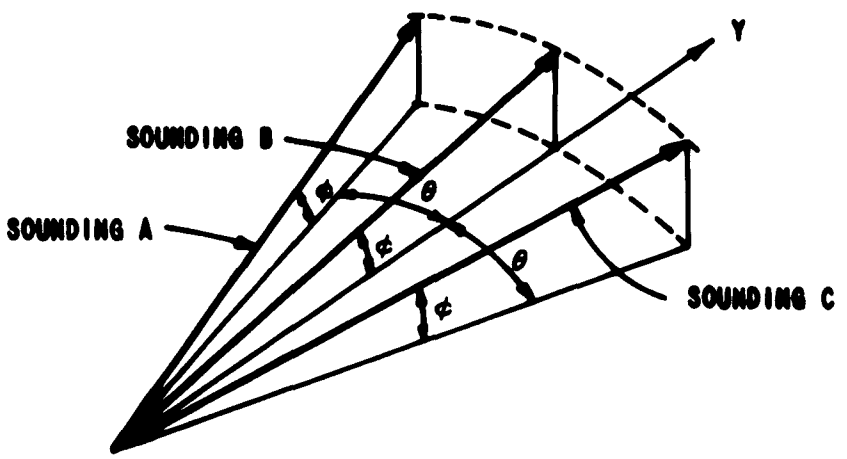

Fig. A-5 - Sounding Geometry of Single Steerable-Probe System

then the soundings give velocity information which may be represented by

$$a = v_s + \bar{W} \cdot \bar{A} \ ;$$

$$b = v_s + \bar{W} \cdot \bar{B} \ ; \text{ and}$$

$$c = v_s + \bar{W} \cdot \bar{C} \ . \qquad \text{(A-16)}$$

The unit vectors are obtained by referring to the diagram of Fig. A-5.

$$\bar{A} = -\cos \phi \sin \theta \, \bar{i} + \cos \phi \cos \theta \, \bar{j} + \sin \phi \, \bar{k} \ ;$$

$$\bar{B} = \cos \phi \, \bar{j} + \sin \phi \, \bar{k} \ ;; \text{ and}$$

$$\bar{C} = \cos \phi \sin \theta \, \bar{i} + \cos \phi \cos \theta \, \bar{j} + \sin \phi \, \bar{k} \ . \qquad \text{(A-17)}$$

Substituting these values into (A-16),

$$a = v_s - W_x \cos \phi \sin \theta + W_y \cos \phi \cos \theta + W_z \sin \phi \ ;$$

$$b = v_s + W_y \cos \phi + W_z \sin \phi \ ; \text{ and}$$

$$c = v_s + W_x \cos \phi \sin \theta + W_y \cos \phi \cos \theta + W_z \sin \phi \ . \qquad \text{(A-18)}$$

Since W_z is small and the sines of the elevation angles are also small, the W_z terms may be neglected, leaving the result:

$$a = v_s - W_x \cos \phi \sin \theta + W_y \cos \phi \cos \theta \ ;$$

$$b = v_s + W_y \cos \phi \ ; \text{ and}$$

$$c = v_s + W_x \cos \phi \sin \theta + W_y \cos \phi \cos \theta \ . \qquad \text{(A-19)}$$

This set of three simultaneous equations may be solved to give the wind velocity components as follows:

$$W_x = \frac{c - a}{2 \cos \phi \sin \theta}$$

$$W_y = \frac{a + c - 2b}{2 \cos \phi (\cos \theta - 1)} \ . \qquad \text{(A-20)}$$

2. Errors in the calculated wind velocity components: In general, each sounding results in a reading (a, b or c) which is in error by some amount e. The elevation angle ϕ is small, so its cosine is nearly equal to unity. The errors* in the calculated wind velocity components are then:

$$\Delta(W_x) \leq \left| \frac{e}{\sin \theta} \right| ; \text{ and}$$

$$\Delta(W_y) \leq \left| \frac{2e}{\cos \theta - 1} \right| . \qquad \text{(A-21)}$$

The values of these errors are plotted as functions of θ in Fig. A-6. The error in the range component W_y is considerably larger than that in the cross-wind component W_x. The significance of the curves may be illustrated by an example: suppose $\theta = 45°$ and $e = 0.5$ mph. Then the errors in the respective wind velocity components are

$$\Delta(W_x) \leq 1.41\, e \text{ (approx. 0.7 mph) ; and}$$

$$\Delta(W_y) \leq 6.85\, e \text{ (approx. 3.4 mph) .}$$

Soundings with an accuracy of $\pm$ 0.5 mph require determining the Doppler shift to about 1 part in 1,500, since the velocity of propagation of the sound wave contributes about 750 mph to the velocity being sensed.

An additional error is contributed by the terms in W_z which were neglected in solving (A-18). This is more than just a question of an unknown vertical wind component, for the presence of the vertical component introduces an error into the calculated values of the other components if (A-20) is used. Studies[6] have shown that the vertical component of wind velocity may in some cases be as high as 5 mph. In such a situation, the neglected terms have values of about 1 mph for an elevation angle of 12°. This will set a lower limit on the error occurring in these measurements, unless a fourth sounding is used so that W_z may also be calculated. Unfortunately, the likelihood of encountering such vertical wind velocities at low altitudes is not known accurately.

* If the errors in the soundings were random, the errors in the calculated wind components could be determined as the square root of the sum of the squares of the errors in the individual soundings. At present, however, there is no basis for expecting random errors, so simple addition of errors has been used.

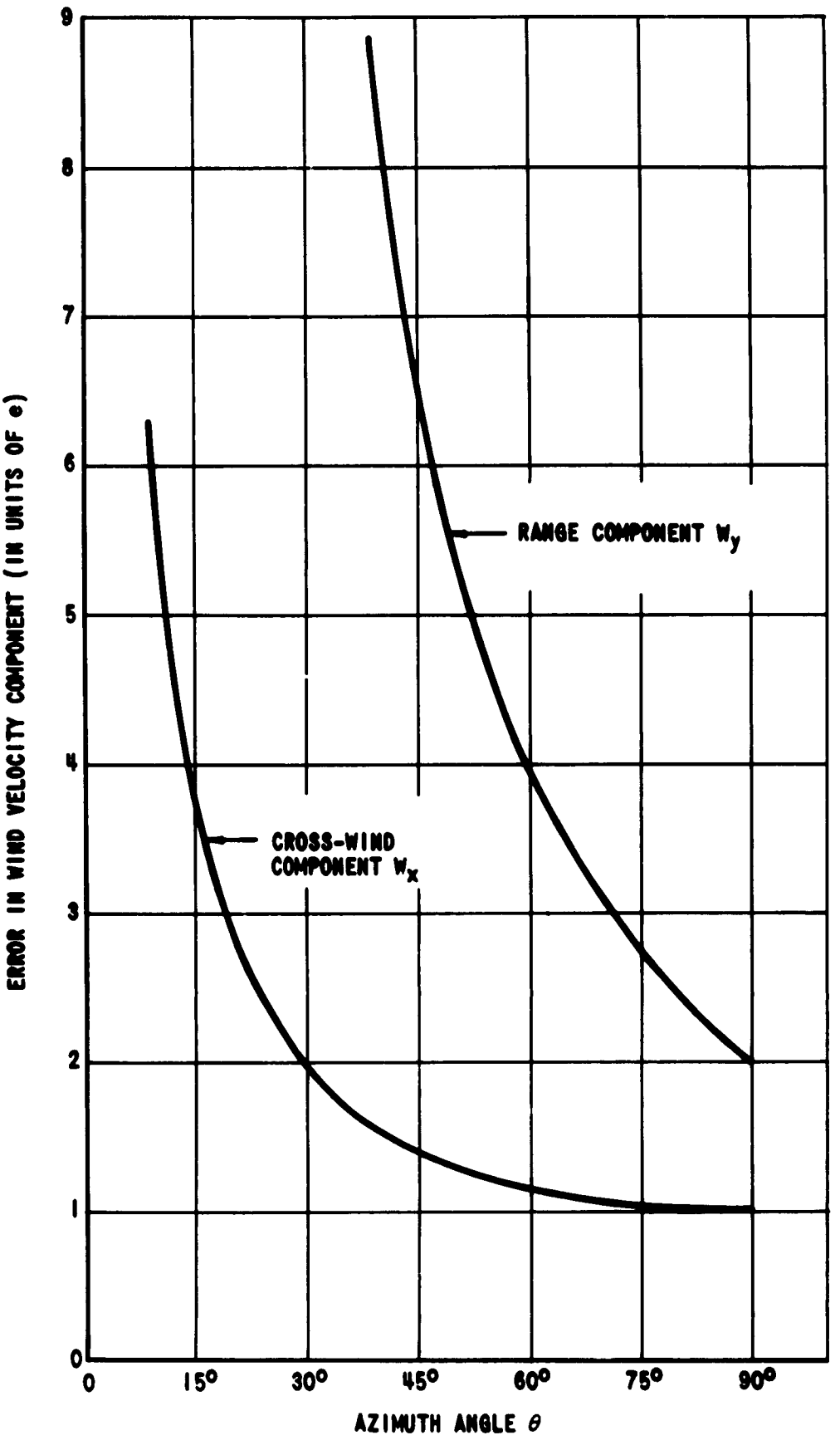

Fig. A-6 - Errors in Wind Velocity Components Determined from Three Soundings with a Single EMAC Probe

In the above analysis, data from the three soundings were combined so as to eliminate the v_s terms of (A-19). Inspection of (A-19) for b, however, shows that if a good estimate of v_s is available, the error in W_y would be equal to the sum of e and the error in v_s. Under such a condition, error in range component is the same as that discussed later in Section II-D-2 of this Appendix.

3. Discussion of the single-probe system: The single-probe system has the obvious advantage of requiring only one EMAC probe, in contrast to the multi-probe systems described in Sections II-C, D and E. In addition, no provisions for scanning the flight path with the single probe are required. Each of the three soundings is made with a fixed azimuth angle (determined by the choice of θ) and a fixed elevation angle (dependent upon the flight path chosen).

The major objection to the use of the single-probe system arises because (as can be seen from Fig. A-6) large values of θ must be used if good accuracy is to be obtained. Consequently, the data gathered by soundings A and C come from points rather far removed from the desired location. For example, if $\theta = 30°$ is selected as giving sufficient accuracy in the calculated wind velocity components; then for a point at range r from the probe, the wind velocity components will be calculated from data obtained at one point on the path and two other points at a distance l, from the first one, where

$$l = 2r \sin 15° , \qquad \text{(A-22)}$$

as illustrated in Fig. A-7. When $r = 1{,}000$ ft., then $d = 520$ ft.; so that two of the soundings are made at points separated by 1,000 ft. While (A-18) contains the implicit assumptions that both the wind velocity, $\bar{W}$, and acoustic propagation velocity, v_s, remain constant during the time interval in which the soundings are made and have the same value for all three sounding points, it appears quite likely that with separations as great as the range, r, these assumptions may not be valid. A statistical approach might give useful information over a given time interval but has not been considered in this study. The distance between outer soundings could be reduced by decreasing the angle θ, but the errors in calculated wind velocities will increase as shown in Fig. A-6.

If the relatively low accuracy of the single-probe system can be tolerated, the system would be attractive because of its simplicity. The multi-probe systems described below require rather careful siting which may be difficult to accomplish under many conditions.

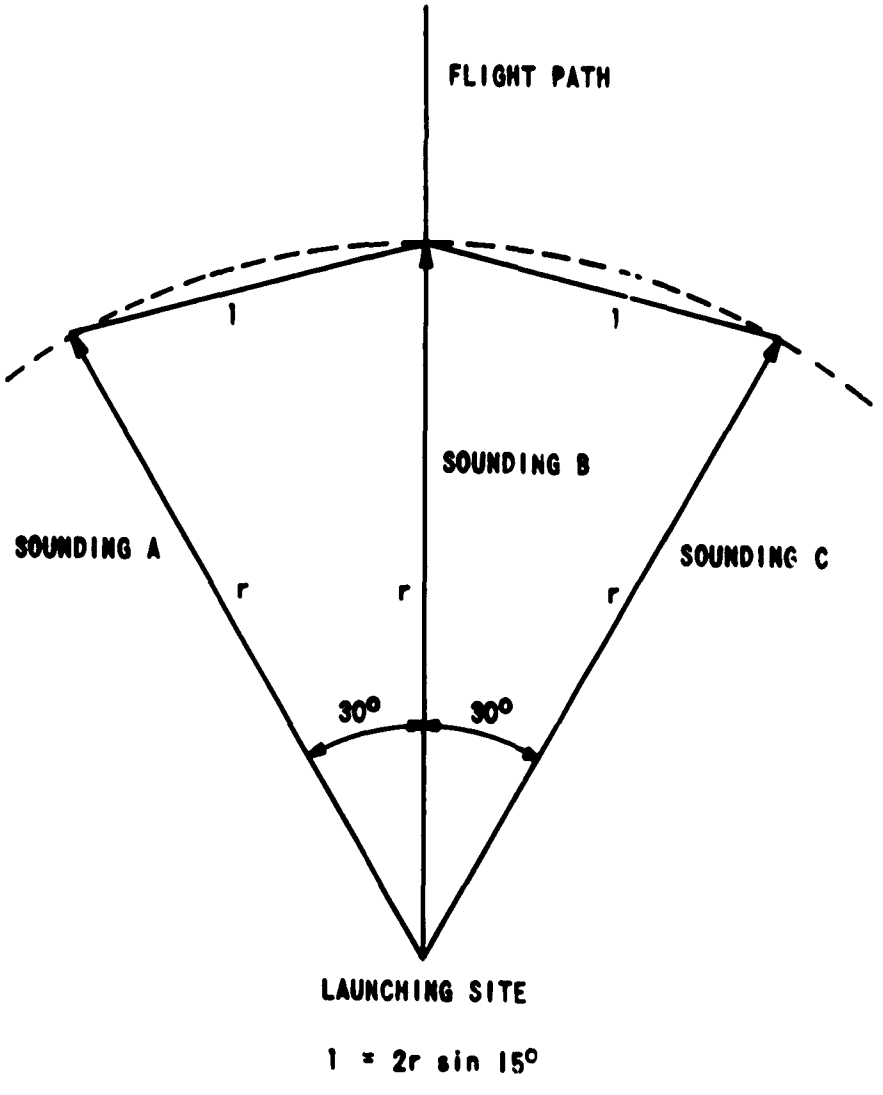

Fig. A-7 - Typical Distances between Soundings and Desired Point for Single-Probe System

C. System Using One Fixed and Two Steerable EMAC Probes

A second method of obtaining the two horizontal wind velocity components consists of taking the three soundings with three different EMAC probes operating from independent sites. A configuration for such a system is shown schematically in Fig. A-8; the location of the two side probes B and C at a distance $r/2$ down the path represents an obvious but rather arbitrary choice.

1. Method for obtaining wind velocity components: For measurements made when the wind vector at some point is $\bar{W}$, (A-15), the soundings give velocity information which is represented by (A-16). In the three-probe case, the unit vectors may be obtained with reference to Fig. A-9 as:

$$\bar{A} = \cos \phi \, \bar{j} + \sin \phi \, \bar{k} \; ;$$

$$\bar{B} = \cos \gamma \cos \theta \, \bar{i} + \cos \gamma \sin \theta \, \bar{j} + \sin \gamma \, \bar{k} \; ; \text{ and}$$

$$\bar{C} = - \cos \gamma \cos \theta \, \bar{i} + \cos \gamma \sin \theta \, \bar{j} + \sin \gamma \, \bar{k} \; . \qquad \text{(A-23)}$$

Substituting these values into (A-16),

$$a = v_s + W_y \cos \phi + W_z \sin \phi \; ;$$

$$b = v_s + W_x \cos \gamma \cos \theta + W_y \cos \gamma \sin \theta + W_z \sin \gamma \; ; \text{ and}$$

$$c = v_s - W_x \cos \gamma \cos \theta + W_y \cos \gamma \sin \theta + W_z \sin \gamma \; . \qquad \text{(A-24)}$$

Again, for small values of W_z and small angles of elevation, the W_z terms may be neglected. This leaves

$$a = v_s + W_y \cos \phi \; ;$$

$$b = v_s + W_x \cos \gamma \cos \theta + W_y \cos \gamma \sin \theta \; ; \text{ and}$$

$$c = v_s - W_x \cos \gamma \cos \theta + W_y \cos \gamma \sin \theta \; . \qquad \text{(A-25)}$$

These equations may be solved to give the wind velocity components as follows:

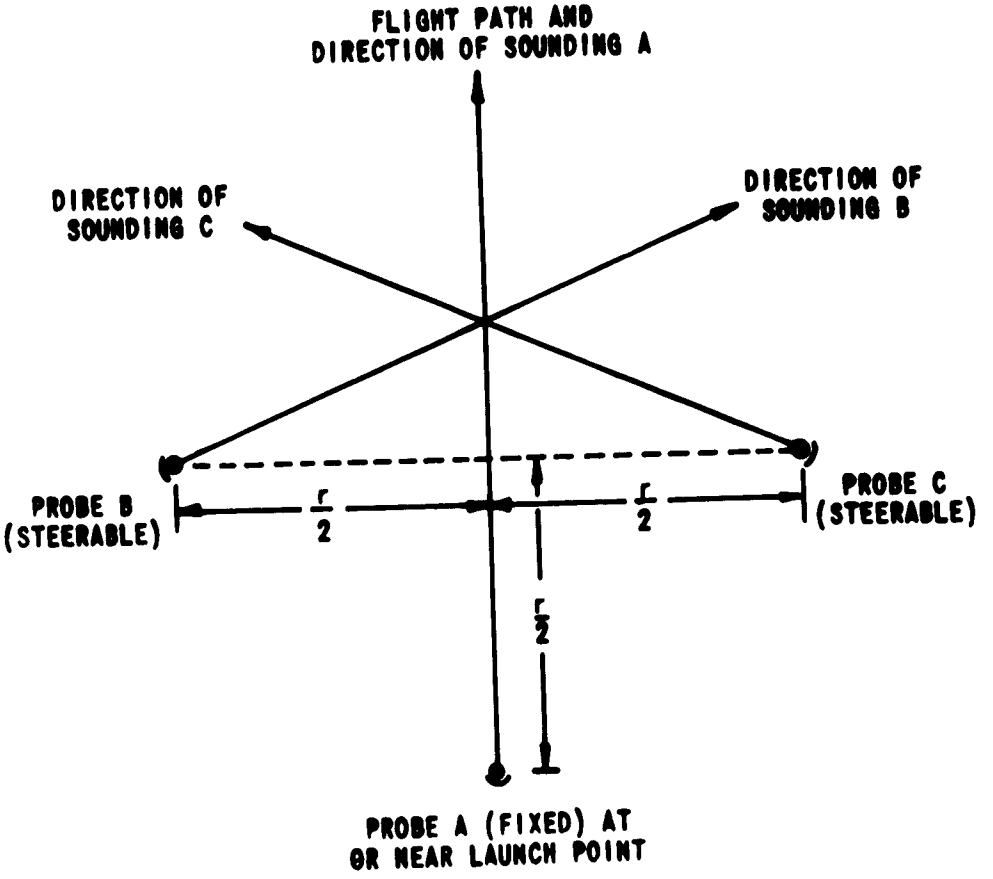

Fig. A-8 - Probe Siting Arrangement for Three-Probe System

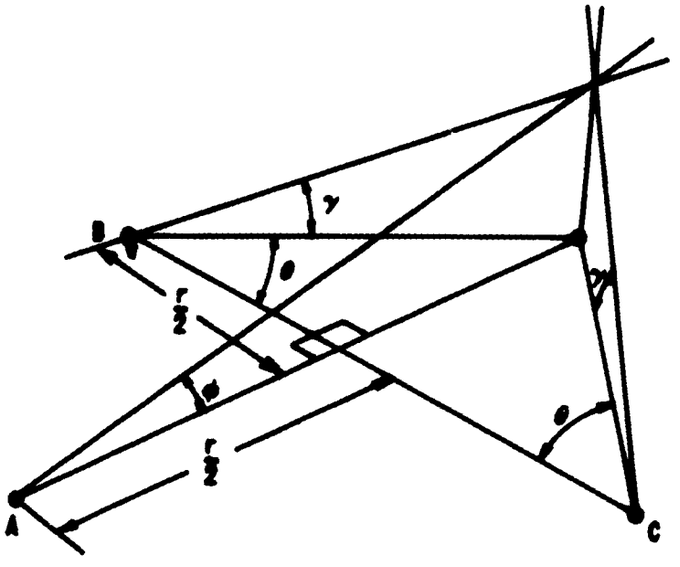

Fig. A-9 - Coordinate System for Three-Probe Configuration

$$W_x = \frac{b - c}{2 \cos \gamma \cos \theta} \quad ;$$

$$W_y = \frac{b + c - 2a}{2(\cos \gamma \sin \theta - \cos \phi)} \qquad \text{(A-26)}$$

2. Errors in the calculated wind velocity components: Each sounding yields a reading (a, b or c) which is in error by some amount e . The cosines of the elevation angles (ϕ , γ) are nearly equal to unity if the angles are small. Therefore, the errors in the calculated wind velocity components are approximately:

$$\Delta(W_x) \leq \left| \frac{e}{\cos \theta} \right| \quad ;$$

$$\Delta(W_y) \leq \left| \frac{2e}{\sin \theta - 1} \right| \quad . \qquad \text{(A-27)}$$

The values of these errors are plotted as functions of θ in Fig. A-10; in this system the value of θ is not fixed, but must be swept through the range -45° to +45° to cover the entire flight path. This must be acccmplished by scanning the flight path with probes B and C .

The intepretation of these curves is illustrated by the following example. Assume that a low-angle path is used, and that e = 0.5 mph ; the errors in the calculated wind velocity components at various points of the path are given in Table A-IV.

TABLE A-IV

TYPICAL ERRORS IN WIND VELOCITY COMPONENTS DETERMINED BY A THREE-PROBE SYSTEM

Position	$\Delta(W_x)$	$\Delta(W_y)$
Launch Point (θ = -45°)	1.41 e ≈ 0.7 mph	1.17 e ≈ 0.6 mph
Mid-Range, $\frac{r}{2}$ (θ = 0°)	1.0 e ≈ 0.5 mph	2 e ≈ 1.0 mph
End of Range, r (θ = +45°)	1.41 e ≈ 0.7 mph	6.85 e ≈ 3.4 mph

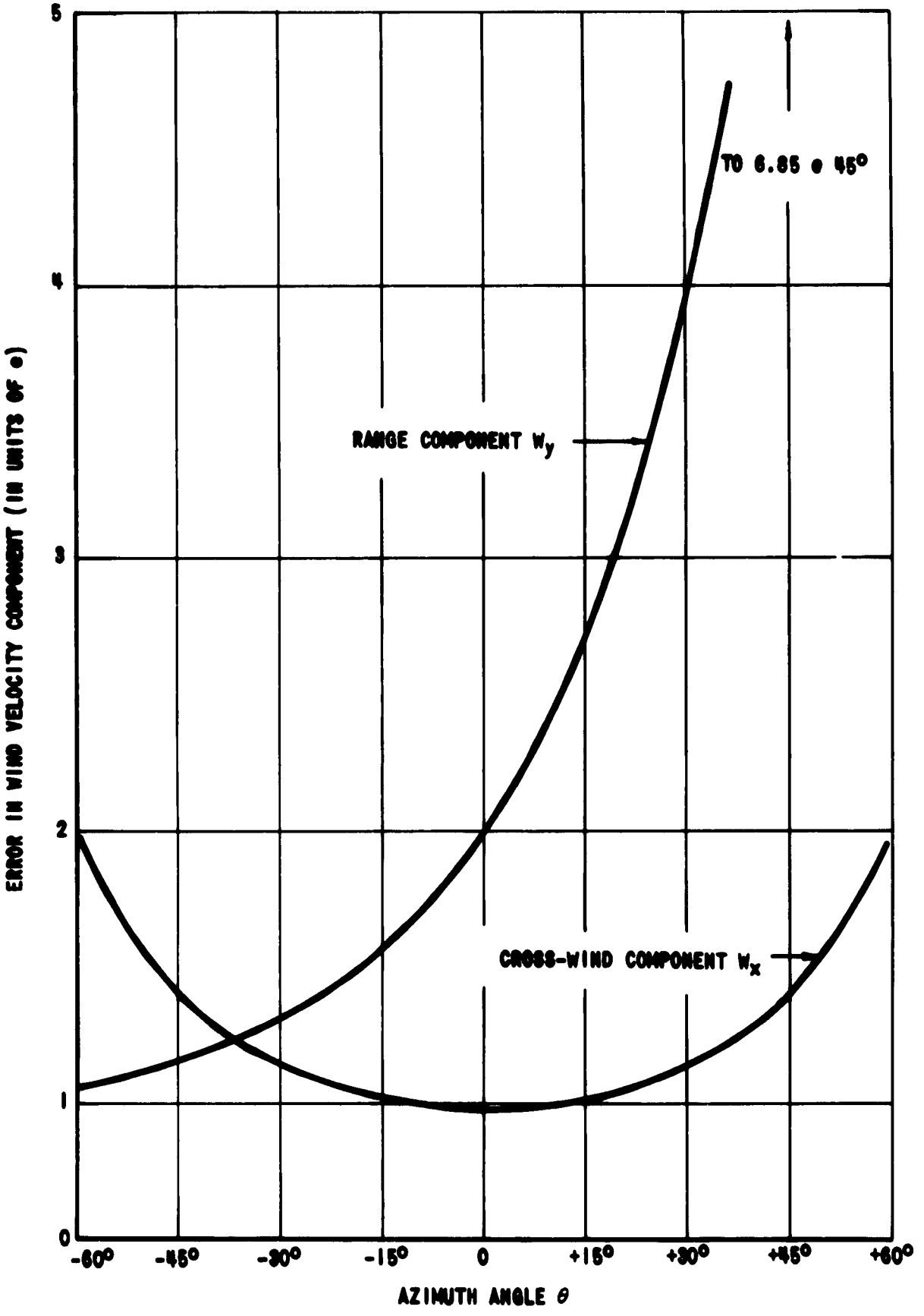

Fig. A-10 - Errors in Wind Velocity Components Determined by Three-Probe System

As in the case of the single-probe system, an error is contributed when the terms in W_z in (A-24) are neglected. The same considerations as to the magnitude of this error apply in the three-probe case.

3. Relationship between sounding angles: The elevation angle γ will be dependent upon the other two angles θ and ϕ. With the aid of Fig. A-9 the relationship among these angles may be found to be

$$\gamma = \tan^{-1}\left[\tan \phi \, (\sin \theta + \cos \theta)\right] . \qquad \text{(A-28)}$$

Provision must be made when scanning the flight path with probes B and C to maintain this relationship between the elevation angle γ and the azimuth angle θ.

4. Discussion of the three-probe system: The arrangement using three EMAC probes is attractive for the measurement of wind profiles along low-elevation trajectories because all the data used in calculating the wind velocity components at a point come from measurements at that point. No assumptions concerning uniformity of the wind velocity over extended distances are necessary, in contrast to the situation in the case of the single-probe system.

D. Substitution of Direct Temperature Measurements for One of the Soundings

If the velocity of sound is assumed to be constant over the path for which the wind velocity profile is to be determined, then its value may be determined by a measurement at one point along the path. Only two additional pieces of data are needed to calculate the wind velocity components; these may be obtained by soundings made with only two EMAC probes.

The only variable which has a significant effect on the velocity of sound in air under usual conditions is the temperature of the air.[7] The rate of change of the velocity of sound with respect to temperature change is about 0.75 mile per hour per degree Fahrenheit. Since the rate of change of air temperature with height is normally about 0.55°F per 100 ft.[8] for heights not too close to the ground, the error resulting from the assumption of constant temperature along the path will not preclude its application for low-elevation angles where, at the maximum range of the EMAC system, the height of the sounding is only a few hundred feet. The measurement of air temperature may be made at the probe site by a thermocouple or other suitable element, or the local sound velocity may be measured directly by electronic means.

1. Method of obtaining wind velocity components: To obtain the two required soundings, only two EMAC probes, say A and B of Fig. A-8, need be used. The velocity information obtained by these two probes has been previously calculated in (A-25):

$$a = v_s + W_y \cos \phi \ ;$$

$$b = v_s + W_x \cos \gamma \cos \theta + W_y \cos \gamma \sin \theta \ . \qquad \text{(A-29)}$$

The third "equation" gives v_s directly in terms of the measured temperature:[7]

$$v_s = (717.3 + 0.75\ T) \text{ mph} \ . \qquad \text{(A-30)}$$

The wind velocity components calculated from these equations are:

$$W_x = \frac{b}{\cos \gamma \cos \theta} - a \frac{\tan \theta}{\cos \phi} + v_s \left(\frac{\tan \theta}{\cos \phi} - \frac{1}{\cos \gamma \cos \theta} \right) \ ; \text{ and}$$

$$W_y = \frac{a - v_s}{\cos \phi} \ . \qquad \text{(A-31)}$$

2. Errors in the two-probe method: In addition to the error e in the soundings, an error δ in the measured velocity of sound in introduced by the assumption that the temperature (and hence v_s) is constant along the flight path. If the cosines of the elevation angles ϕ and γ are approximately equal to unity, then the approximate errors in the velocity components are:

$$\Delta(W_x) \leq \left| \frac{e\ (1 + |\sin \theta|)}{\cos \theta} \right| + \left| \frac{\delta(1 + \sin \theta)}{\cos \theta} \right| \ ; \text{ and}$$

$$\Delta(W_y) \leq \left| e + \delta \right| \ . \qquad \text{(A-32)}$$

Errors in the temperature sensing instrument are included in δ .

The size of the errors involved may be illustrated by means of an example: suppose that $e = 0.5$ mph, and that the error introduced as δ corresponds to 2°F, or 1.5 mph. The errors in the calculated wind velocity components along the path are shown in Fig. A-11. The errors introduced by neglecting the vertical component of the wind velocity have not been included.

3. Discussion of the two-probe system: The two-probe system offers a modest improvement in simplicity over the three-probe system. However, the assumption of constant temperature along the flight path results in larger errors in the calculated wind-velocity components. Whether the sacrifice in accuracy offsets the reduced complexity of the system must be subjectively decided.

The use of a sound velocity measurement to replace one of the soundings may be particularly attractive in adapting the three-probe system to tactical applications.

III. REFERENCES USED IN THIS APPENDIX

1. Denman, E., "Air Velocity Sensing," (Unclassified), Proceedings of Progress Report Symposium, ANIP, 1959; Bell Document No. D228-100-003 (Confidential), pp. 257-261.

2. Kerr, D. E., Propagation of Short Radio Waves, McGraw-Hill Book Company, Inc., New York, 1951; Section 3.4, pp. 189-193. See also Hunter, J. L., Acoustics, Prentice-Hall, Inc., Englewood Cliffs, N. J., 1957; Section 3.3, pp. 888-91.

3. Hunter, op. cit., pp. 298-300.

4. Pollard, E. C., and Sturtevant, J. M., Microwaves and Radar Electronics, John Wiley & Sons, Inc., New York, 1948; p. 244.

5. Condon, E. V., and Odishaw, H., Handbook of Physics, McGraw-Hill Book Company, Inc., New York, 1958, pp. 3-121.

6. Brown, W. D., Parachutes, Sir Isaac Pitman & Sons, London, 1951; p. 13.

7. Beranek, L. L., Acoustic Measurements, John Wiley & Sons, Inc., New York, 1949; p. 47.

8. Sutton, O. G., Micrometeorology, McGraw-Hill Book Company, Inc., New York, 1953; pp. 7-13 and pp. 190-192.

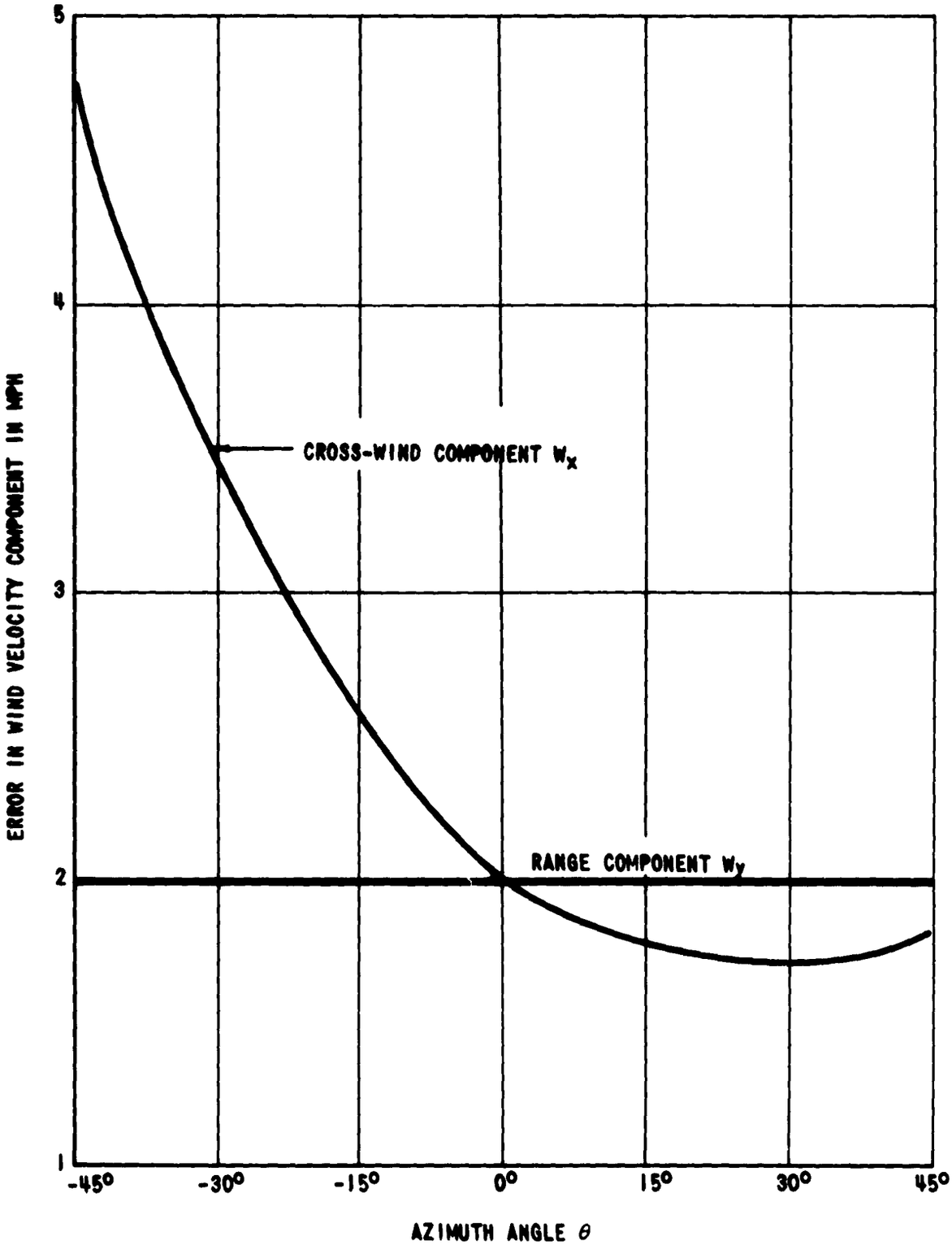

Fig. A-11 - Typical Errors in Wind Velocity Components Determined by the Two-Probe System

APPENDIX B

ANALYSIS OF A HEATED BUBBLE OF GAS IN THE FREE ATMOSPHERE

I. THERMODYNAMIC BEHAVIOR

A quantitative assessment of the behavior of a bubble of heated gas in the atmosphere is undertaken below in terms of the simplest form of modeling. The bubble is to be released at ground level and its motion, shape, temperature and density are determined up to 1500 meters. A simple derivation of each relationship is presented as well as a numerical evaluation. There are three treatments for each relationship corresponding to assumed temperature lapse rates for the atmosphere.

As stated before, the most simple form of model is used for this investigation in order to provide estimates of the thermodynamic quantities. Individual assumptions and simplifications can certainly be questioned with respect to their validity in the real world; however it is felt that meaningful conclusions can be drawn with respect to feasibility of infrared tracking of the heated bubble as a consequence of this study.

A. Assumed Model

The essential description of the model is given below.

1. Turbulent and molecular diffusion effects on the shape or energy content of the bubble are neglected.

2. Radiational exchange between the bubble and its environment are not permitted.

3. The thermodynamic processes occurring in the bubble are strictly adiabatic in nature.

4. The atmosphere is in static equilibrium and exerts no shear or drag forces on the bubble which can modify its shape or influence its motion.

5. The atmosphere can be characterized by a uniform temperature gradient. In this investigation there are three gradients assumed: isothermal, -1°C/100 meters, and -2°C/100 meters.

B. Equations Used in Derivations of the Thermodynamic Relationships

The equations that will be used in this derivation are:

1. The hydrostatic equation for the atmosphere:

$$\frac{dp}{dZ} = -g\rho \quad , \tag{B-1}$$

where p is pressure,

Z is height,

g is acceleration of gravity, and

ρ is density of air.

2. The perfect gas law:

$$p = R\rho T \quad , \tag{B-2}$$

where p is pressure,

R is universal gas constant/molecular weight,

ρ is density, and

T is absolute temperature.

3. The first law of thermodynamics:

$$dQ = C_v \, dT + A \, p d\left(\frac{1}{\rho}\right) \quad , \tag{B-3}$$

where dQ is amount of heat exchanged across boundaries of system/unit mass,

C_v is specific heat at constant volume,

dT is differential temperature change,

A is the reciprocal of mechanical equivalent of heat,

p is pressure, and

$d\left(\frac{1}{\rho}\right)$ is the differential change in volume.

4. Characterization of the free atmosphere:

$$T_a = T_{ao} - cZ \quad , \tag{B-4}$$

where T_a is temperature of the atmosphere at any point in °K,

T_{ao} is temperature of the atmosphere at $Z = 0$,

c is the lapse rate in °C/100 meters, and

Z is the height in meters.

C. Derivations of Thermodynamic Relationships

1. Determination of bubble temperature: The differential of (B-2) is

$$pd\left(\frac{1}{\rho}\right) = RdT - \frac{dp\ RT}{p} \quad . \tag{B-5}$$

Substituting (B-5) into (B-3) yields

$$dQ = (C_v + AR)dT - ART\frac{dp}{p} \quad . \tag{B-6}$$

Also, $AR = C_p - C_v$ where C_p is specific heat at constant pressure, hence,

$$dQ = C_p\ dT - (C_p - C_v)\ T\frac{dp}{p} \quad . \tag{B-7}$$

Since $\gamma = \frac{C_p}{C_v}$ and $dQ = 0$ for adiabatic case, (B-7) becomes

$$\frac{dT}{T} = \frac{\gamma-1}{\gamma}\frac{dp}{p} \quad . \tag{B-8}$$

Substituting $\rho = \frac{p}{RT}$ from (B-2) in (B-1) yields

$$\frac{dp}{p} = -\frac{g}{RT}\,dZ \quad . \tag{B-9}$$

Substituting (B-9) in (B-8) and assuming $p_a = p_b$:

$$\frac{d\,T_b}{T_b} = -\frac{\gamma_b-1}{\gamma_b}\frac{g}{R_a T_a}\,dZ \quad , \tag{B-10}$$

where T_b is temperature of the bubble.

For an isothermal atmosphere, $T_a = T_{ao}$ = constant, the solution of (B-10) is

$$T_b = T_{bo}\exp\left[-\frac{g}{R_a T_{ao}}\left(\frac{\gamma_b-1}{\gamma_b}\right)\right]Z \quad . \tag{B-11}$$

For finite lapse rate, $T_a = T_{ao} - \alpha Z$, the solution of (B-10) is

$$T_b = T_{bo}\left(1 - \frac{\alpha Z}{T_{ao}}\right)^{\left(\frac{g}{\alpha R_a}\right)\left(\frac{\gamma_b-1}{\gamma_b}\right)} \tag{B-12}$$

The ratio, T_b/T_{bo} , of bubble temperature at height Z to its temperature at the ground is tabulated in Table B-I for various heights and lapse rates, α .

TABLE B-I

RATIOS OF BUBBLE TEMPERATURES

	Z(meters)								
α(°C/100 meters)	0	200	400	600	800	1000	1200	1400	1500
0	1	0.999	0.986	0.981	0.974	0.967	0.962	0.954	0.952
1	1	0.993	0.987	0.98	0.973	0.967	0.96	0.953	0.95
2	1	0.994	0.987	0.98	0.973	0.966	0.96	0.953	0.95

2. Determination of atmospheric density: The differential of (B-2) is

$$dp = R(Td\rho + \rho dT) \quad . \tag{B-13}$$

Substituting (B-13) into (B-1) yields

$$\frac{d\rho}{\rho} = -\frac{1}{T}\left(\frac{dT}{dZ} + \frac{g}{R}\right)dZ \quad . \tag{B-14}$$

For an isothermal atmosphere, $T = T_{ao}$ and $\frac{dT}{dZ} = 0$, the solution of (B-14) is

$$\rho_a = \rho_{ao} \exp\left(-\frac{g}{T_{ao}R_a} Z\right) \quad . \tag{B-15}$$

For finite lapse rate, $T_a = T_{ao} - \alpha Z$, the solution of (B-14) is

$$\rho_a = \rho_{ao}\left(1 - \frac{\alpha Z}{T_{ao}}\right)^{\left(\frac{g}{R_a\alpha} - 1\right)} \quad . \tag{B-16}$$

The ratio, ρ_a/ρ_{ao} , of the atmospheric density at height Z to its density at the ground is tabulated in Table B-II for various heights and lapse rates, α .

TABLE B-II

RATIOS OF ATMOSPHERIC DENSITIES

	Z(meters)								
α(°C/100 meters)	0	200	400	600	800	1000	1200	1400	1500
0	1	0.978	0.957	0.935	0.914	0.893	0.873	0.853	0.844
1	1	0.983	0.969	0.953	0.936	0.923	0.907	0.891	0.884
2	1	0.991	0.981	0.972	0.963	0.953	0.943	0.934	0.929

3. Determination of density of bubble: It is assumed that at all levels $P_a = P_b$. From (B-2),

$$\rho_a R_a T_a = \rho_b R_b T_b \quad ,$$

or

$$\rho_b = \rho_a \frac{R_a}{R_b} \frac{T_a}{T_b} \quad . \tag{B-17}$$

For an isothermal atmosphere, substitution of (B-11) and (B-15) into (B-17) yields

$$\rho_b = \frac{R_a}{R_b} \frac{T_{ao}}{T_{bo}} \rho_{ao} \exp\left(-\frac{gZ}{T_{ao} R_a \gamma_b}\right) \quad .$$

But

$$\rho_{bo} = \frac{R_a}{R_b} \frac{T_{ao}}{T_{bo}} \rho_{ao} \quad ,$$

therefore

$$\rho_b = \rho_{bo} \exp\left(-\frac{gZ}{T_{ao} R_a \gamma_b}\right) . \qquad \text{(B-18)}$$

For finite lapse rate, substitution of (B-12) and (B-16) into (B-17) yields

$$\rho_b = \rho_{bo}\left(1 - \frac{\alpha Z}{T_{ao}}\right)^{\frac{g}{R_a \alpha \gamma_b}} . \qquad \text{(B-19)}$$

The ratio, ρ_b/ρ_{bo} , of the bubble density at height Z to its density at the ground is tabulated below in Table B-III for various heights and lapse rates, α .

TABLE B-III

RATIOS OF BUBBLE DENSITIES

	Z(meters)								
α(°C/100 meters)	0	200	400	600	800	1000	1200	1400	1500
0	1	0.985	0.969	0.954	0.938	0.923	0.908	0.895	0.887
1	1	0.983	0.969	0.953	0.936	0.923	0.907	0.891	0.884
2	1	0.984	0.967	0.952	0.936	0.919	0.904	0.889	0.88

4. Determination of solid angle: The solid angle, Ω , subtended at the ground by the bubble is porportional to the projected area of the bubble divided by Z^2 . Assuming that the bubble is spherical, the solid angle can be represented by

$$\Omega \propto \frac{(\text{vol})^{2/3}}{Z^2} ,$$

since vol $\propto 1/p$, Ω can be expressed as

$$\Omega \propto \frac{\left(\frac{1}{\rho_b}\right)^{2/3}}{Z^2} \quad . \tag{B-20}$$

The ratio, Ω/Ω_0 , of the solid angle subtended at the ground by the bubble at height Z to the angle subtended by the bubble at 100 meters is tabulated in Table B-IV for various heights and lapse rates, α .

TABLE B-IV

RATIOS OF SOLID ANGLES

	Z(meters)								
α(°C/100 meters)	100	200	400	600	800	1000	1200	1400	1500
0	1	0.252	0.063	0.029	0.016	0.011	0.007	0.006	0.005
1	1	essentially same as above							
2	1								

5. Determination of bubble height dependence on time: This is approached as a buoyant force calculation where

$\rho_a v_a g$ = weight of air ,

$\rho_b v_b g$ = weight of bubble , and

$v_a = v_b = v$.

Therefore

$(\rho_a - \rho_b)vg$ = net force on bubble, and

$$(\rho_a - \rho_b)gv = \rho_b v \frac{d^2Z}{dt^2} \quad ,$$

or

$$\frac{d^2Z}{dt^2} = \left(\frac{\rho_a}{\rho_b} - 1\right) g \quad . \tag{B-21}$$

For an isothermal atmosphere, substitution of (B-15) and (B-18) into (B-21) yields

$$\frac{d^2Z}{dt^2} = g\left[\left(\frac{\rho_{ao}}{\rho_{bo}} \exp\left(-\frac{g(\gamma_b-1)}{T_{ao}R_a\gamma_b} Z\right)\right) - 1\right] \quad . \tag{B-22}$$

For finite lapse rate, substitution of (B-16) and (B-19) into (B-21) yields

$$\frac{d^2Z}{dt^2} = g\left[\frac{\rho_{ao}}{\rho_{bo}}\left(1 - \frac{\alpha Z}{T_{ao}}\right)^{\left[\frac{g(\gamma_b-1)}{R_a\alpha\gamma_b} - 1\right]} - 1\right] \quad . \tag{B-23}$$

The time (in seconds) required for the bubble to rise from the ground to height Z is tabulated in Table B-V for various combinations of density ratio, ρ_{bo}/ρ_{ao}, and lapse rate, α. (The $\rho_{bo} = 0.75\ \rho_{ao}$ corresponds roughly to an initial temperature difference of 100°C.)

TABLE B-V

BUBBLE RISE TIMES

α(°C/100 meters)	ρ_{bo}/ρ_{ao}	Z(meters) 0	200	400	600	800	1000	1200	1400
0	0.75	0	11.28	15.95	19.5	22.6	25.3	27.8	30.1
0	0.85	0	15.68	22.15	27.00	31.35	35.15	38.6	41.9
0	0.95	0	30.1	42.6	52.4	60.9	68.8	76.8	83.8
1	0.75	0	11.1	15.7	19.2	22.2	24.8	27.15	29.3
1	0.85	0	15.28	21.6	26.5	30.6	34.2	37.4	40.4
1	0.95	0	28.35	40.0	49.0	56.6	63.3	69.4	75.0
2	0.75	0	10.91	15.45	18.89	21.79	24.34	26.64	28.7
2	0.85	0	14.87	21.0	25.7	29.65	33.05	36.15	28.95
2	0.95	0	26.8	37.85	46.3	53.1	58.8	63.9	68.5

II. THE INFRARED DETECTION SYSTEM

A. Proposed System

In order to detect the radiation from the gas in the bubble by a passive infrared search system, it is necessary that the gas bubble emit strongly in the infrared spectrum. A number of gases emit radiation in the infrared spectrum, some of which are constituents of the atmosphere. A good choice for the heated gas of the bubble would be a mixture of carbon dioxide and dry air. The essential properties of the mixture are that it contains as much carbon dioxide as possible and it must always be less dense than the atmosphere. The carbon dioxide, and therefore the bubble, will radiate as a black body in narrow wavelength intervals corresponding to the absorption wavelengths. However, since it is richer in carbon dioxide than the atmosphere and has a higher partial pressure of CO_2, the bubble will radiate over a wider band of wavelengths than the atmosphere due to pressure broadening. Thus, if the detection system is adjusted to accept a narrow band of wavelengths located just to one side of the CO_2 absorption band of the atmosphere as shown in Fig. B-1, the CO_2 in the atmosphere will not absorb much of the energy radiated by the bubble in that narrow band. The atmosphere will be transparent to the desired radiation providing that none of the other constituents of the atmosphere absorb energy in the band of wavelengths accepted by the detection system.

The choice of wavelength accepted by the detection system is determined by the absorption band of CO_2 which is used. A wavelength for which the atmosphere is transparent but is next to a carbon dioxide absorption wavelength would be the most desirable wavelength at which to operate. A suitable choice would be 4.1 microns which is on the sharp edge of the 4.3 micron absorption band of carbon dioxide. The atmosphere has no constituents which absorb energy at this wavelength, consequently it is transparent at this wavelength.

Since 4.1 microns is a favorable wavelength for propagation, the next consideration is the availability of suitable detectors. In the selection of a suitable detector, the major factors to be considered are sensitivity and optimum signal-to-noise ratio. In these considerations, all the incoming radiation is treated as signal and the noise referred to is that generated in the photoconductor. Available detectors have a D* of about 10^{10}. An estimate of the signal-to-noise ratio can be made by considering a detector with dimensions 1 mm. x 1 mm. using a 90 cycle per second chopper to modulate the incoming radiation, a 5 cycle amplifier bandwidth, and liquid nitrogen cooling. A signal-to-noise ratio of approximately 55 db. would be obtained by this system. This would indicate that detector noise will be no problem in this application.

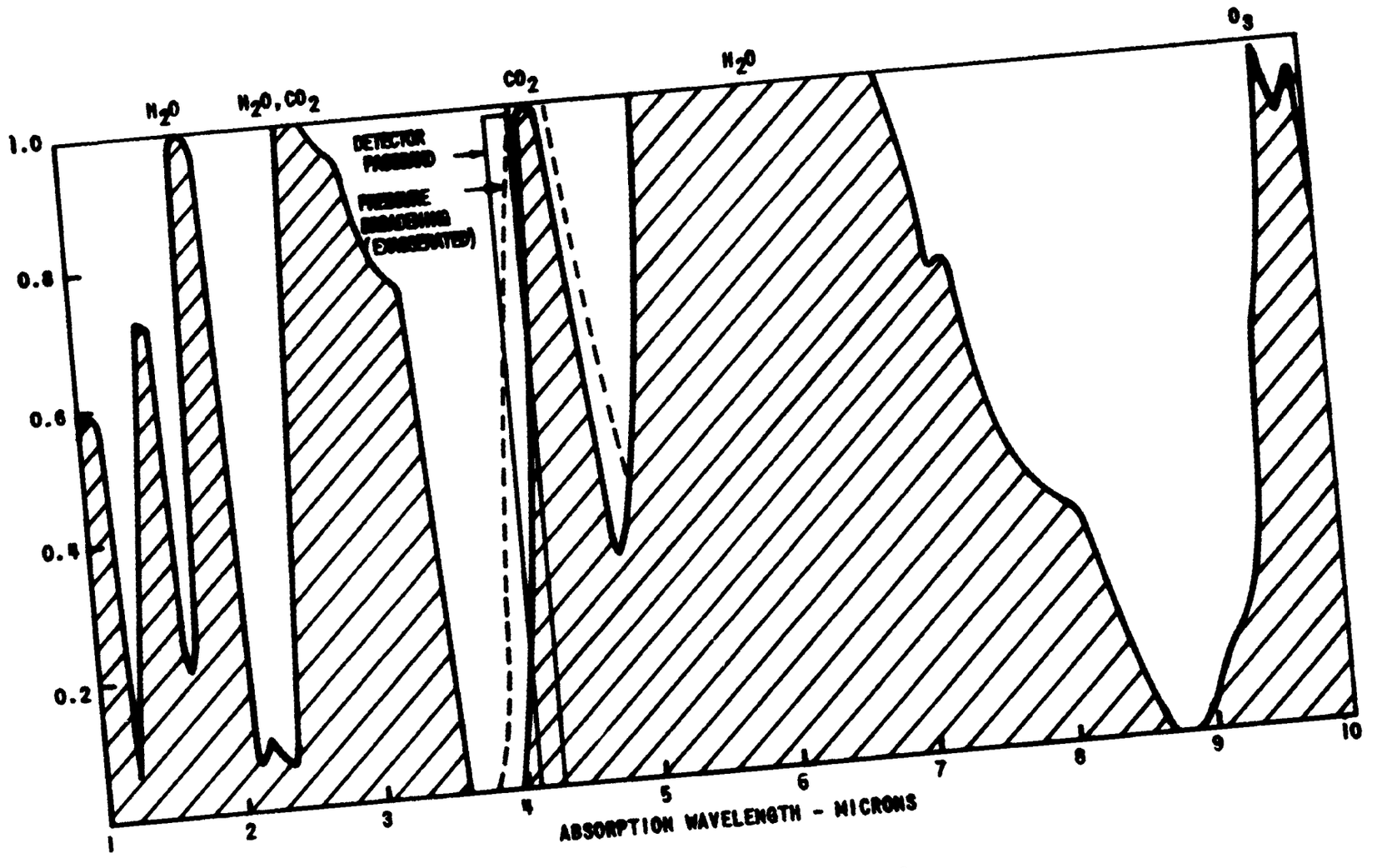

Fig. B-1 - Atmospheric Absorption Bands

The significant noise in this system will be due to the radiation from the background. The system should be sufficiently flexible so that the sun will never shine directly on the detector system, thus the noise radiance will be from other sources. An estimate of this noise is 0.1 to 2 w/meter^2-steradian-micron. The value could be easily determined experimentally.

B. Radiance at Earth's Surface from Bubble

The intensity of the radiation from the bubble of gas at a temperature T is given by the equation

$$I(\lambda,T) = \frac{C_1}{\lambda^5} \frac{1}{\left[e^{+C_2/\lambda T}-1\right]} \quad \text{watts/meter}^2\text{/micron} \ , \qquad \text{(B-24)}$$

where $C_1 = 3.74 \times 10^8$ watts micron^4/meter^2 ,

$C_2 = 1.439 \times 10^4$ micron °K , and

λ = wavelength in microns.

The total power emitted by the bubble is

$$W(\lambda,T) = I(\lambda,T)4\pi r_b^2 \ , \qquad \text{(B-25)}$$

where r_b is the radius of the bubble.

The radiant emittance at the earth's surface from a bubble of temperature T located at a height Z above the earth's surface is

$$I(\lambda,T,r,Z) = I(\lambda,T)\ r_b^2/Z^2 \ . \qquad \text{(B-26)}$$

The radius of the bubble is not independent of the bubble temperature so the r_b^2 dependence in (B-26) must be removed. Using the perfect gas law and the approximation $R_b \approx R_a \cong R$,

$$r_b^2 = \left[\frac{3\, M_b\, R\, T_b}{4\pi\, p_b}\right]^{2/3} \quad . \qquad \text{(B-27)}$$

Substituting (B-24) and (B-27) in (B-26), for 4.1 microns, $I(\lambda,T,r,Z)$ becomes

$$I(\lambda,T,Z) = \frac{3.23 \times 10^5}{e^{\frac{3510}{T_b}} - 1} \left[\frac{3}{4}\,\frac{1}{\pi}\,\frac{M_b}{\rho_a}\right]^{2/3} \left[\frac{T_b}{T_a}\right]^{2/3} \frac{1}{Z^2} \quad , \qquad \text{(B-28)}$$

using the relations $p_a = p_b$ and $p_a = \rho_a R T_a$. Using an $M_b = 30$ gm. , $\rho_a = 1000$ gm/m^3 as average values, a plot of the radiance at the earth's surface from a bubble at 1500 meters versus the difference between the bubble temperature and the air temperature is shown in Fig. B-2 for three values of the air temperature at 1500 meters. The calculations for the data in this figure are given in Table B-VI.

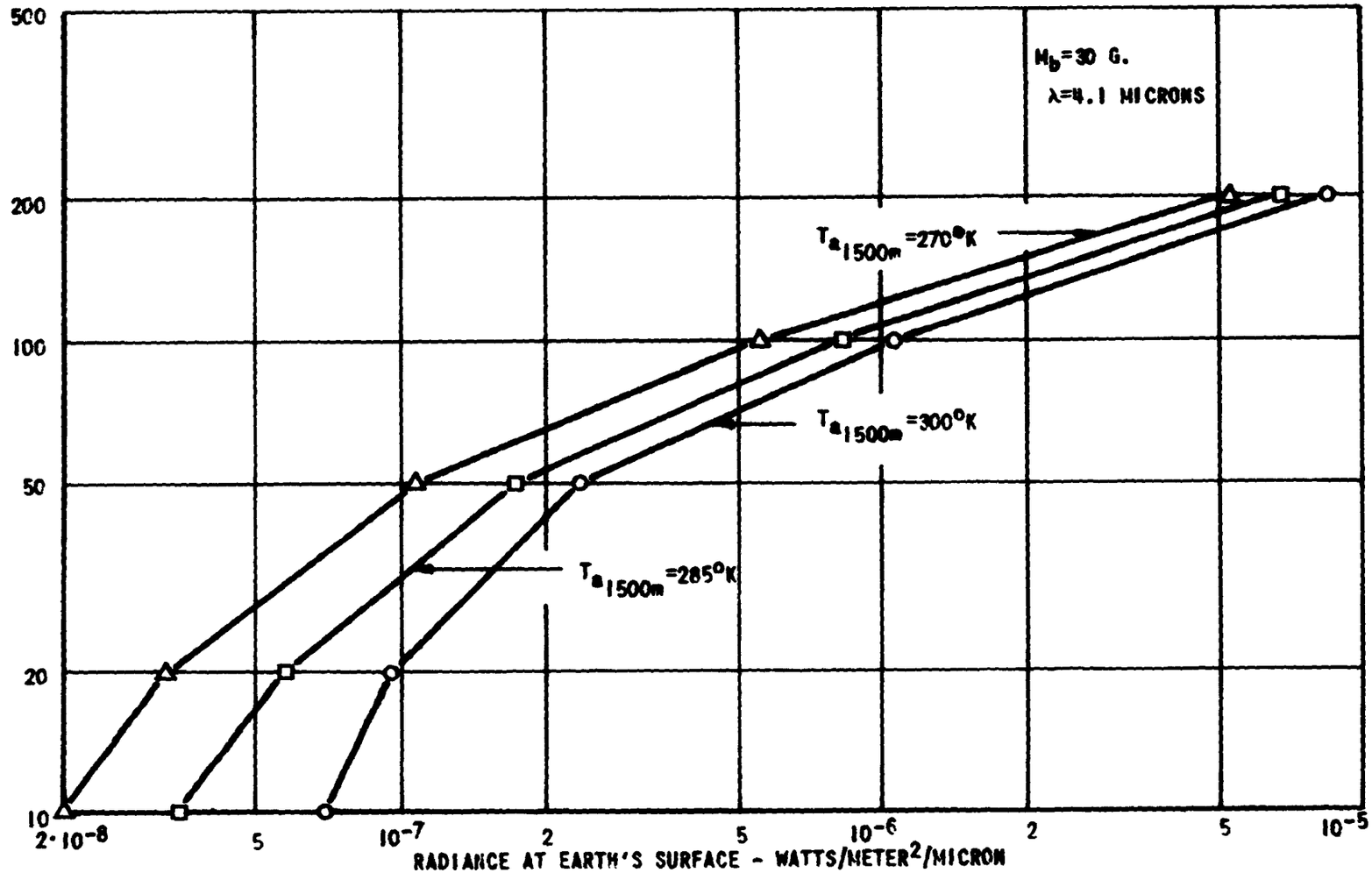

Fig. B-2 - Radiance from Bubble at 1,500 Meters Above Earth's Surface

TABLE B-VI

CALCULATIONS OF RADIANCE AT THE EARTH'S SURFACE FROM A BUBBLE OF TEMPERATURE $T_b = T_a + \Delta T$ AT 1500 METERS ABOVE THE EARTH'S SURFACE

(λ = 4.1 Microns)

$$I(4.1\mu, T, 1500m) = 5.38 \times 10^{-3} \left[\frac{T_b}{T_a}\right]^{2/3} \frac{1}{e^{\frac{3510}{T_b}} - 1}$$

ΔT °K	$\frac{3510}{T_b}$	T_b/T_a	$(T_b/T_a)^{2/3}$	$e^{\frac{3510}{T_b}} - 1$	$(T_b/T_a)^{2/3} \Big/ e^{\frac{3510}{T_b}} - 1$	$I(4.1\mu, T_b, 1500m)$
	For $T_{a_{1500m}} = 300°K$			$T_b = T_a + \Delta T$		(Isothermal)
10	11.3	1.035	1.023	80,000	1.28×10^{-5}	6.9×10^{-8}
20	11.0	1.07	1.046	60,000	1.78×10^{-5}	9.6×10^{-8}
50	10.0	1.165	1.104	22,000	5.3×10^{-5}	2.85×10^{-7}
100	8.77	1.33	1.22	6,500	2.05×10^{-4}	1.1×10^{-6}
200	7.0	1.67	1.41	1,100	1.53×10^{-3}	8.2×10^{-6}
	For $T_{a_{1500m}} = 285°K$				(Adiabatic Lapse Rate)	
10	11.9	1.035	1.023	160,000	6.4×10^{-6}	3.44×10^{-8}
20	11.5	1.07	1.046	100,000	1.07×10^{-5}	5.77×10^{-8}
50	10.5	1.175	1.114	37,000	3.17×10^{-5}	1.72×10^{-7}
100	9.1	1.35	1.22	9,000	1.5×10^{-4}	8.2×10^{-7}
200	7.25	1.70	1.42	1,400	1.21×10^{-3}	6.65×10^{-6}
	For $T_{a_{1500m}} = 270°K$				(Twice Adiabatic Lapse Rate)	
10	12.5	1.035	1.023	280,000	3.67×10^{-6}	1.98×10^{-8}
20	12.1	1.075	1.05	180,000	6×10^{-6}	3.23×10^{-8}
50	11.0	1.185	1.12	60,000	1.97×10^{-5}	1.06×10^{-7}
100	9.5	1.37	1.23	13,000	1.05×10^{-4}	5.65×10^{-7}
200	7.48	1.74	1.45	1,800	9.65×10^{-4}	5.2×10^{-6}

III. EVALUATION OF THE ASSUMPTION OF NEGLIGIBLE RADIATION LOSS

The thermodynamic model used in the preceding analysis has been based on the assumption of negligible loss of energy by thermal radiation. Yet the infrared detection and tracking system cannot operate without the existence of detectable amounts of this radiation. The purpose of this section is to examine this inconsistency. The approach taken will be to use the results of the infrared detection analysis to determine the amount of radiation required, and then to determine whether or not this amount of radiation would be significant in the thermodynamic analysis.

From the infrared analysis, it has been established that a 30-gm. bubble, to be detectable at a height of 1,500 meters, must be some 200°K above the temperature of the surrounding air. It has also been established that the bubble temperature, in degrees Kelvin, does not change significantly as the bubble rises from ground level up to the 1,500-meter level. Hence, a good first approximation is to assume that the bubble temperature is constant for the calculation of energy loss by radiation.

Assuming in addition that the bubble radiates as a black body at all wavelengths, the rate of loss of energy by radiation to the surroundings would be

$$\frac{dQ}{dt} = \sigma A_b (T_b^4 - T_a^4) \quad , \tag{B-29}$$

where $\frac{dQ}{dt}$ = rate of energy loss, watts;

σ = the Stefan-Boltzmann constant, 5.67×10^{-8} watts/$m^2(°K)^4$;

A_b = surface area of the bubble, m^2;

T_b = temperature of the bubble, °K; and

T_a = temperature of the surrounding air, °K.

The surface area of the bubble is related to its temperature and pressure. The radius of the bubble has been computed from the ideal gas law as

$$r_b = \left[\frac{3\ M_b R_b T_b}{4\pi P_b}\right]^{1/3} , \qquad \text{(B-30)}$$

where M_b = mass of gas in the bubble, kg.;

R_b = universal gas constant ÷ molecular weight of gas, ≈287 joule/kg °K if molecular weight = 29; and

P_b = pressure of gas in the bubble, newtons per m^2.

If the bubble is assumed to be in pressure equilibrium with its surroundings, then

$$P_b = P_a = \rho_a R_a T_a , \qquad \text{(B-31)}$$

where P_a = air pressure, newtons/m^2;

ρ_a = air density, kg/m^3;

$R_a \approx R_b$; and

T = air temperature, °K.

Consequently,

$$r_b = \left[\frac{3\ M_b T_b}{4\pi \rho_a T_a}\right]^{1/3} , \qquad \text{(B-32)}$$

and the surface area of the bubble is

$$A_b = 4\pi r_b^2 = 4\pi \left[\frac{3\ M_b T_b}{4\pi \rho_a T_a}\right]^{2/3} . \qquad \text{(B-33)}$$

In order to obtain numerical values, take the following case:

$T_b = 500°K$;

$T_a = 300°K$;

$M_b = 0.030$ kg. = 30 gm. ; and

$\rho_a = 0.85\ \rho_{ao}$ (corresponding to the isothermal case at Z = 1500 m)

$= 1.09\ kg/m^3$.

Then

$$\frac{dQ}{dt} = (5.67 \times 10^{-8}) 4\pi \left[\frac{3(0.030)(500)}{4\pi(1.09)(300)} \frac{kg\ °K\ m^3}{kg\ °K} \right]^{2/3}$$

$$\times \left[(500)^4 - (300)^4 \right] \frac{watts\ (°K)^4}{m^2\ (°K)^4} = 1.910\ watts\ . \qquad \text{(B-34)}$$

The total energy radiated from the bubble during its ascent is

$$Q_{tot} = \frac{dQ}{dt} \cdot t_a\ , \qquad \text{(B-35)}$$

where t_a = ascent time to 1,500 meters (seconds). Calculations for the rate of rise of the heated bubble indicate that a bubble heated to 500°K would reach 1,500 meters in about 20 sec. Hence

$$Q_{rad} = 1{,}910 \text{ watts x } 20 \text{ sec.} = 38{,}200 \text{ joules}\ . \qquad \text{(B-36)}$$

Now to ascertain whether this loss of energy by radiation is significant in the thermodynamic model, this energy may be compared with the total energy initially stored in the bubble. Assuming the bubble is heated at constant volume to 500°K, the total energy input is

$$Q_{in} = M_b C_v \Delta T = (0.030 \text{ kg}) \left(716 \frac{\text{joules}}{\text{kg } ^\circ\text{K}}\right) (200^\circ\text{K}) = 4{,}300 \text{ joules} \qquad \text{(B-37)}$$

Hence, it is quite evident by comparing Q_{rad} and Q_{in} that radiation losses are not negligible. In fact, they appear so large that the system would be almost unworkable under the assumed conditions. However, it must be pointed out that the gas bubble has been assumed to be radiating as a black body at all wavelengths, which is not correct and results in overestimating the energy loss by radiation. It seems reasonable to conclude, however, that the heated bubble concept will not be usable up to altitudes of 1,500 meters. If a usable working range for this system is needed, a more detailed analysis taking radiation losses into account in the thermodynamic model will be required.

DISTRIBUTION LIST

Contract No. DA 36-039 SC-87293

No. of Copies	Recipient
1	Office of Assi· ant Secretary of Defense, (R & E), Room 3E1065 The Pentagon Washington 25, D. C. Attn: Technical Library
1	Chief of Research and Development OCS, Department of the Army Washington 25, D. C.
1	Chief Signal Officer Department of the Army Washington 25, D. C. Attn: SIGRD
1	Chief Signal Officer Department of the Army Attn: SIGCO Washington 25, D. C.
1	Chief Signal Officer Attn: SIGAC Department of the Army Washington 25, D. C.
1	Chief Signal Officer Attn: SIGPL Department of the Army Washington 25, D. C.
1	Director U. S. Naval Research Laboratory Attn: Code 2027 Washington 25, D. C.
1	Commanding Officer and Director U. S. Navy Electronics Laboratory San Diego 52, California

DISTRIBUTION LIST (Continued)

No. of Copies	Recipient
1	U. S. National Bureau of Standards Boulder Laboratories Attn: Library Boulder, Colorado
2	Headquarters Aeronautical Systems Division Attn: WCOSI-3 Wright-Patterson Air Force Base, Ohio
1	Commander Air Force Cambridge Research Center Attn: CROTR Bedford, Massachusetts
1	Commander Rome Air Development Center Attn: RCSSLD Griffiss Air Force Base, New York
1	Commanding General U. S. Army Electronic Proving Ground Fort Huachuca, Arizona
10	Commander Armed Services Technical Information Agency Attn: TIPDR Arlington Hall Station Arlington 12, Virginia
1	Commanding Officer U. S. Army Signal Eqp. Support Agency Fort Monmouth, New Jersey Attn: SIGFM/ES-ADJ
1	Corps of Engineers Liaison Office U. S. Army Signal R & D Laboratory Fort Monmouth, New Jersey

DISTRIBUTION LIST (Continued)

No. of Copies	Recipient
1	Marine Corps Liaison Office U. S. Army Signal R & D Laboratory Fort Monmouth, New Jersey
1	Commanding Officer U. S. Army Signal R & D Laboratory Attn: Director of Research Fort Monmouth, New Jersey
1	Commanding Officer U. S. Army Signal R & D Laboratory Attn: Technical Documents Center Fort Monmouth, New Jersey
1	Commanding Officer U. S. Army Signal R & D Laboratory Attn: SIGRA/SL-ADJ, File Unit #3 Fort Monmouth, New Jersey
5	Commanding Officer U. S. Army Signal R & D Laboratory Fort Monmouth, New Jersey Attn: Technical Information Division
2	Chief, U. S. Army Security Agency Arlington Hall Station Arlington 12, Virginia
1	Deputy President U. S. Army Security Agency Board Arlington Hall Station Arlington 12, Virginia
1	Commanding Officer U. S. Army Signal Missile Support Agency Missile Geophysics Division Redstone Arsenal, Alabama
1	Commander Air Force Cambridge Research Center Attn: CRZC, Dr. M. R. Nagel L. G. Hanscom Field Bedford, Massachusetts

DISTRIBUTION LIST (Continued)

No. of Copies	Recipient
1	Director Atmospheric Sciences Programs National Science Foundation Washington 25, D. C.
1	Office of Naval Research Department of the Navy Washington 25, D. C.
1	The University of Texas Electrical Engineering Research Laboratory Austin, Texas
1	American Meteorological Society Abstracts and Bibliography P.O. Box 1736 Washington 13, D. C.
1	New York University Meteorology Department University Heights New York 53, New York
1	Library U. S. Weather Bureau Washington 25, D. C.
1	Signal Corps Liaison Office Massachusetts Institute of Technology 77 Massachusetts Avenue Building 26, Room 131 Cambridge 39, Massachusetts
1	Brookhaven National Laboratories Camp Upton, New York
1	Mr. Jack Pierrard Armour Research Foundation Chicago, Illinois

DISTRIBUTION LIST (Concluded)

No. of Copies	Recipient
1	Mr. Harry Moses Radiological Physics Division Argonne National Laboratory 9700 South Cass Avenue Argonne, Illinois
1	Dr. David Atlas Chief, Weather Radar Branch GRD AFCRL Weather Radar Field Site Sudbury, Massachusetts
24	Transportation Officer for Activity Supply Officer U. S. Army Signal R & D Laboratory Logistics Division Bldg. 2504, Charles Wood Area Fort Monmouth, New Jersey Marked for: SIGRA/SL-SMI Contract No. DA 36-039 SC-87293

AD_____

Midwest Research Institute, Kansas City, Mo. INVESTIGATION OF TECHNIQUES FOR REMOTE MEASUREMENT OF ATMOSPHERIC WIND FIELDS, R.W.Fetter, P.L.Smith,Jr., B.L.Jones, H.C.Schick, R.M. Stewart,Jr. Report No. 2, 77 pp., 24 illus., 10 tables, Contract DA-36-039 SC-87295, Phase II: Analysis, 15 Oct. 1961 - 14 Feb. 1962. Unclassified Report

Analyses were made to determine the feasibility of three proposed methods of remote wind measurement using (1) scattering from natural atmospheric turbulence, (2) electromagnetic scattering from acoustic waves, and (3) infrared tracking of an artificially heated volume of air or "bubble."

(over)

UNCLASSIFIED

1. Meteorological data -- measurement.
2. Meteorological instruments.
3. Wind -- velocity.
4. Contract No. DA-36-039 SC-87295

UNCLASSIFIED

AD_____

Midwest Research Institute, Kansas City, Mo. INVESTIGATION OF TECHNIQUES FOR REMOTE MEASUREMENT OF ATMOSPHERIC WIND FIELDS, R.W.Fetter, P.L.Smith,Jr., B.L.Jones, H.C.Schick, R.M. Stewart,Jr. Report No. 2, 77 pp., 24 illus., 10 tables, Contract DA-36-039 SC-87295, Phase II: Analysis, 15 Oct. 1961 - 14 Feb. 1962. Unclassified Report

Analyses were made to determine the feasibility of three proposed methods of remote wind measurement using (1) scattering from natural atmospheric turbulence, (2) electromagnetic scattering from acoustic waves, and (3) infrared tracking of an artificially heated volume of air or "bubble."

(over)

UNCLASSIFIED

1. Meteorological data -- measurement.
2. Meteorological instruments.
3. Wind -- velocity.
4. Contract No. DA-36-039 SC-87295

UNCLASSIFIED

AD _____

Midwest Research Institute, Kansas City, Mo. INVESTIGATION OF TECHNIQUES FOR REMOTE MEASUREMENT OF ATMOSPHERIC WIND FIELDS, R.W.Fetter, P.L.Smith,Jr., B.L.Jones, H.C.Schick, R.M. Stewart,Jr. Report No. 2, 77 pp., 24 illus. 10 tables, Contract DA-36-039 SC-87295, Phase II: Analysis, 15 Oct. 1961 - 14 Feb. 1962. Unclassified Report

Analyses were made to determine the feasibility of three proposed methods of remote wind measurement using (1) scattering from natural atmospheric turbulence, (2) electromagnetic scattering from acoustic waves, and (3) infrared tracking of an artificially heated volume of air or "bubble."

(over)

UNCLASSIFIED

1. Meteorological data -- measurement.
2. Meteorological instruments.
3. Wind -- velocity.
4. Contract No. DA-36-039 SC-87295

UNCLASSIFIED

AD _____

Midwest Research Institute, Kansas City, Mo. INVESTIGATION OF TECHNIQUES FOR REMOTE MEASUREMENT OF ATMOSPHERIC WIND FIELDS, R.W.Fetter, P.L.Smith,Jr., B.L.Jones, H.C.Schick, R.M. Stewart,Jr. Report No. 2, 77 pp., 24 illus. 10 tables, Contract DA-36-039 SC-87295, Phase II: Analysis, 15 Oct. 1961 - 14 Feb. 1962. Unclassified Report

Analyses were made to determine the feasibility of three proposed methods of remote wind measurement using (1) scattering from natural atmospheric turbulence, (2) electromagnetic scattering from acoustic waves, and (3) infrared tracking of an artificially heated volume of air or "bubble."

(over)

UNCLASSIFIED

1. Meteorological data -- measurement.
2. Meteorological instruments.
3. Wind -- velocity.
4. Contract No. DA-36-039 SC-87295

UNCLASSIFIED

AD_____ Use of natural turbulence as a sensor will require (1) additional data on distribution and characteristics of turbulence from ground level to one mile altitude, (2) correlation of turbulence motion and wind, and (3) radar state-of-the-art improvement to provide consistent detection and measurement. Remote wind measurements by microwave reflection from acoustic waves have been demonstrated, but additional experimental data are needed to determine maximum usable range and the effects of turbulence on the acoustic waves. Remote generation of a heated bubble of air does not appear feasible.	UNCLASSIFIED UNCLASSIFIED	AD_____ Use of natural turbulence as a sensor will require (1) additional data on distribution and characteristics of turbulence from ground level to one mile altitude, (2) correlation of turbulence motion and wind, and (3) radar state-of-the-art improvement to provide consistent detection and measurement. Remote wind measurements by microwave reflection from acoustic waves have been demonstrated, but additional experimental data are needed to determine maximum usable range and the effects of turbulence on the acoustic waves. Remote generation of a heated bubble of air does not appear feasible.	UNCLASSIFIED UNCLASSIFIED
AD_____ Use of natural turbulence as a sensor will require (1) additional data on distribution and characteristics of turbulence from ground level to one mile altitude, (2) correlation of turbulence motion and wind, and (3) radar state-of-the-art improvement to provide consistent detection and measurement. Remote wind measurements by microwave reflection from acoustic waves have been demonstrated, but additional experimental data are needed to determine maximum usable range and the effects of turbulence on the acoustic waves. Remote generation of a heated bubble of air does not appear feasible.	UNCLASSIFIED UNCLASSIFIED	AD_____ Use of natural turbulence as a sensor will require (1) additional data on distribution and characteristics of turbulence from ground level to one mile altitude, (2) correlation of turbulence motion and wind, and (3) radar state-of-the-art improvement to provide consistent detection and measurement. Remote wind measurements by microwave reflection from acoustic waves have been demonstrated, but additional experimental data are needed to determine maximum usable range and the effects of turbulence on the acoustic waves. Remote generation of a heated bubble of air does not appear feasible.	UNCLASSIFIED UNCLASSIFIED